Nano Energy 136 (2025) 110767

Contents lists available at ScienceDirect

Nano Energy

journal homepage: www.elsevier.com/locate/nanoen

Review

Triboelectric nanogenerators as a practical approach for wind energy harvesting: Mechanisms, designs, and applications

Di Liu [a,1], Jianjun Luo [b,c,1], Lijun Huang [b,c], Muqi Chen [b], Minglan Ji [b,c], Zhong Lin Wang [b,*], Jiahao Kang [a,d,**]

[a] Research Center for Carbon-based Electronics, School of Electronics, Peking University, Beijing 100871, China

[b] Beijing Key Laboratory of Micro-Nano Energy and Sensor, Center for High-Entropy Energy and Systems, Beijing Institute of Nanoenergy and Nanosystems, Chinese Academy of Sciences, Beijing 101400, China

[c] School of Nanoscience and Engineering, University of Chinese Academy of Sciences, Beijing 100049, China

[d] Institute for Carbon-Based Thin Film Electronics, Peking University, Shanxi (ICTFE-PKU), Taiyuan 030012, China

ARTICLE INFO

Keywords:
TENG
Self-powered system
Wind energy
Wind-TENG structural design
Hybrid Wind-TENG-EMG
Power management circuit

ABSTRACT

Constructing self-powered sensors or systems is an effective method to meet the power consumption requirements of millions and billions of distributed electronic devices. As a ubiquitous, clean, and renewable energy source, wind energy plays an important role in power supply. Compared with traditional wind electromagnetic generators, wind triboelectric nanogenerator (wind-TENG) has unique advantages such as lightweight, low cost, and low start-up wind speed, which are more suitable for driving the above-mentioned distributed electronic devices. In this review, the recent progress of wind-TENG from basic working principles to practical applications is systematically summarized. First, the recent progress of wind-TENG in terms of structural design and start-up wind speed is reviewed. Subsequently, the power management principle as well as the related circuit design of the wind-TENG are introduced. Furthermore, the development of self-powered systems based on wind-TENG in agriculture, transportation, and environment monitoring fields is reviewed. Finally, some perspectives and challenges for the future development of wind-TENG are also discussed.

1. Introduction

With the rapid development of electronic technology, sensing technology, and the Internet of Things (IoT), the number of connected terminals is growing exponentially. Millions and billions of sensors or systems will require power, leading to a substantial increase in energy consumption [1]. Since the IoT terminals are often widely distributed, traditional power supply methods, such as cabling, are expensive and difficult to change once installed. The conventional approach of using batteries presents challenges, as they contribute to environmental pollution and require maintenance when depleted [2]. In this context, harvesting energy from the ambient environment and developing self-powered sensors and systems offer practical solutions to meet the energy demands of distributed applications. Ambient energy sources, including solar [3], vibration [4,5], wind [6], and hydroenergy [7], among others [8,9], will play a great role in the power supply for future technologies. Wind energy, in particular, is one of the most important clean and renewable energy sources, contributing approximately 4.3 % of global electricity generation [10]. Given its abundance, wind energy has attracted considerable attention for energy harvesting.

Traditional wind energy harvesting using electromagnetic generators (EMGs) is based on the principle of electromagnetic induction [11] (Fig. 1a). EMGs typically have low impedance, resulting in high current and low voltage output (Fig. 1b). Another promising technology for energy harvesting, the triboelectric nanogenerator (TENG), was proposed in 2012 by Prof. Zhong Lin Wang [12]. It converts the wind energy into electricity based on the triboelectric effect and electrostatic induction [13] (Fig. 1c). The TENG has high voltage, low current, and high impedance output characteristics (Fig. 1d) [14,15]. Notably, the output power per unit volume of TENGs is higher than that of EMGs (Fig. 1e), allowing TENGs to be designed as lightweight, small, and cost-effective devices. Additionally, EMGs exhibit inferior performance at low

* Corresponding author.
** Corresponding author at: The Research Center for Carbon-based Electronics, School of Electronics, Peking University, Beijing 100871, China.
E-mail addresses: zhong.wang@mse.gatech.edu (Z.L. Wang), kang@pku.edu.cn (J. Kang).

[1] These authors contribute equally to this work.

https://doi.org/10.1016/j.nanoen.2025.110767
Received 11 January 2025; Received in revised form 5 February 2025; Accepted 7 February 2025
Available online 10 February 2025

operating frequencies. Compared with EMGs, TENGs show a much better performance at low frequency (typically < 5 Hz) [16] (Fig. 1f), making them highly advantageous for low-frequency wind energy harvesting. Furthermore, TENGs can be fabricated with a wide range of materials, such as films [17–19], rabbit hair [20], fiber [21], metal foil [22], and nanoparticles [23]. This versatility gives TENGs significant potential for self-powered applications across various scenarios.

Recent progress has increasingly focused on the practicability of self-powered applications [24]. A commonly employed strategy involves using triboelectric nanogenerators (TENGs) to charge a capacitor, which then powers the load automatically once sufficient energy is collected. However, given that natural wind conditions are often erratic, intermittent, and sometimes even absent, one of the major challenges is optimizing the device's structural design to reduce the minimum required wind speed for start-up. By achieving lower start-up wind speeds, the energy-harvesting efficiency of TENGs can be significantly enhanced, allowing them to operate more consistently under variable environmental conditions. Additionally, designing a matching power management circuit can dramatically improve energy extraction, accelerate capacitor charging, and ensure automatic system operation. As a result, these technologies stimulate the development of a wide range of TENG-based self-powered applications.

Here in this paper, four basic operating modes of TENGs are firstly introduced. Then, a comprehensive review of wind-TENG structural designs is provided, focusing on configurations optimized for both low and high start-up wind speeds, as well as hybrid wind-TENG-EMG systems (Fig. 2). Following this, recent advancements in power management circuits are summarized, which play a critical role in optimizing energy harvesting efficiency. Furthermore, a series of typical self-powered application scenarios based on wind-TENGs is presented, including applications in agriculture area, transportation area, and environmental monitoring. Lastly, the prospective development and

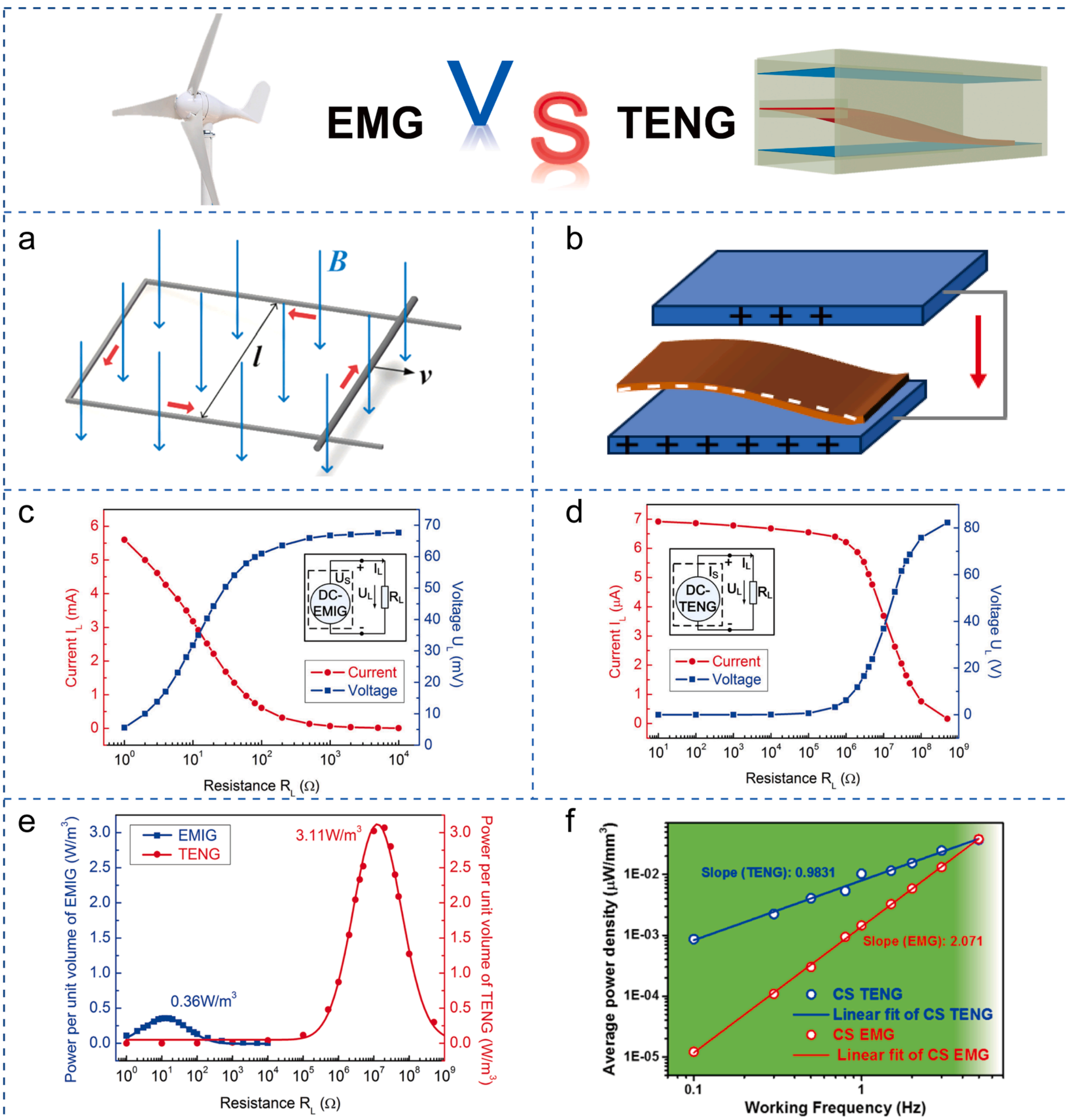

Fig. 1. Comparison between conventional wind-EMG and wind-TENG. (a,b) Illustration of the mechanism of EMG (a) [11] and TENG (b), respectively. (c,d) The output characteristics of EMG (c)[11] and TENG (d). (e–f) Comparison of the TENG and EMIG (electromagnetic induction generator) on the volume (e) [11] and operating frequency (f) [16].
Reproduced with permission.

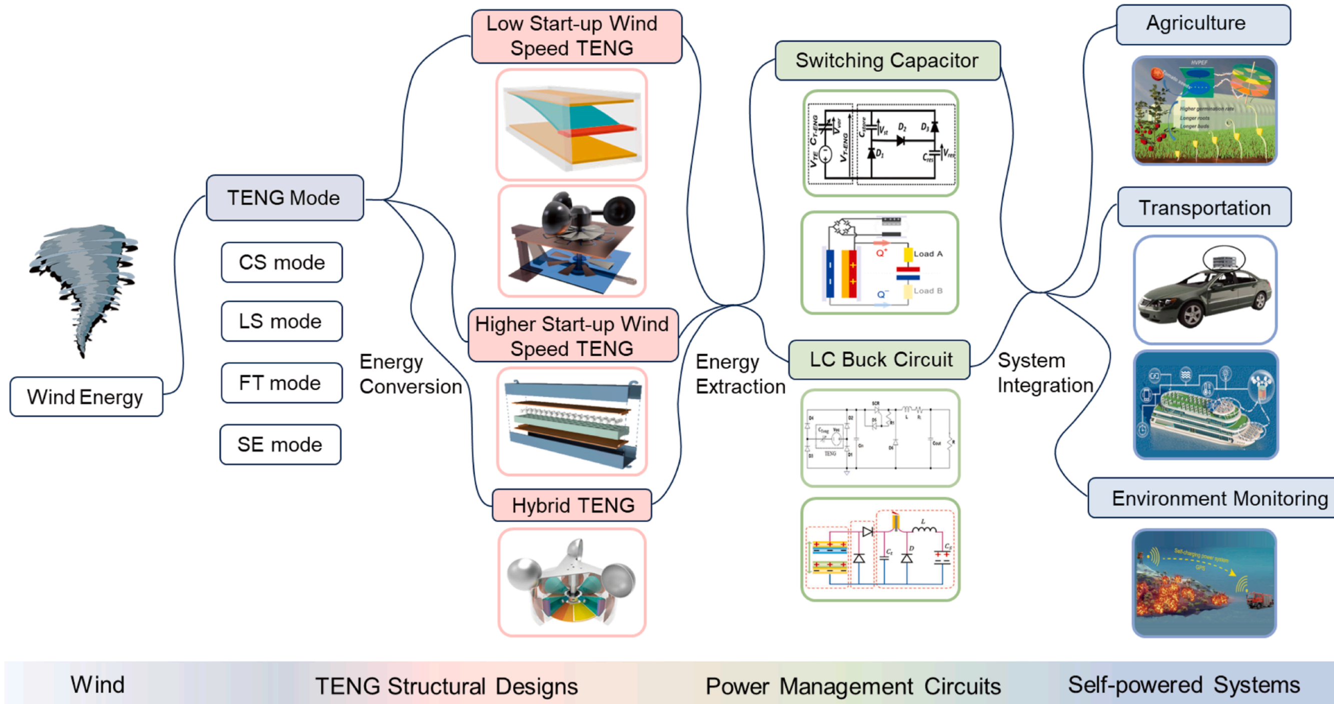

Fig. 2. Mind map for constructing self-powered sensors or systems [17,25–35].

future trends of wind-TENG technology are discussed.

2. Basic working modes of TENG

To develop a more practical structure for wind energy harvesting, the TENG needs to be well designed to minimize the friction resistance and enhance the output performance. There are four basic working modes [36–38] of TENG that can be selected for structural design: contact-separation (CS) mode, literal-slide (LS) mode, single-electrode (SE) mode, and freestanding triboelectric-layer (FT) mode. In the SE and FT modes, the electrodes remain stationary, whereas in the CS and LS modes, they are movable. Despite these differences, the core working mechanism of all four modes is based on forming a variable capacitor within the TENG. According to the capacitive model of TENG [39,40], as the capacitance of the TENG changes, due to the relative movement of the surfaces and electrostatic induction, charges will transferred through the external circuit. This dynamic variation in capacitance drives the energy generation process in each mode, enabling efficient energy conversion in various environments.

As shown in Fig. 3a, CS mode TENG is the most fundamental structure [41] which consists of two plates. Each plate is fabricated by a dielectric layer attached to the metal layer. When two kinds of material

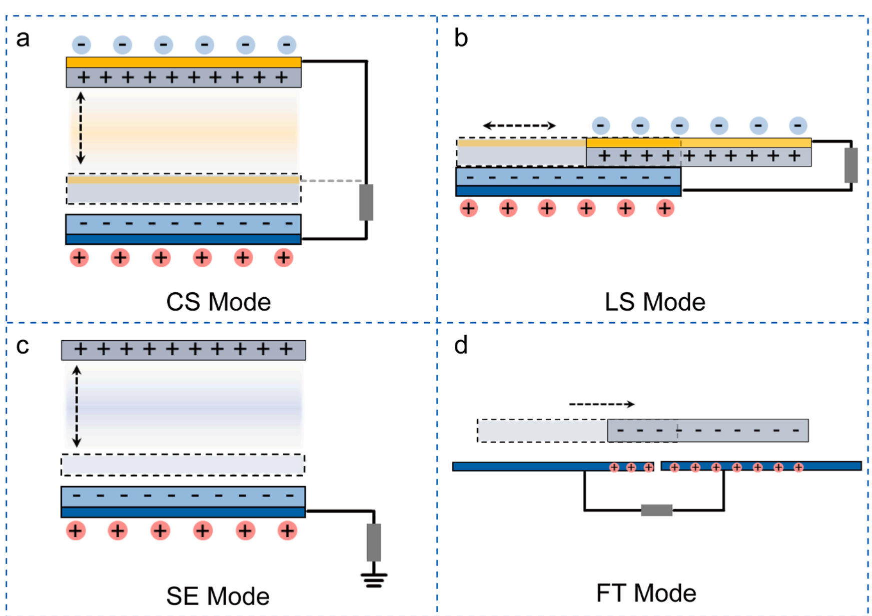

Fig. 3. Four working modes of TENG. (a) Contact-separation (CS) mode. (b) Literal-slide (LS) mode. (c) Single-electrode (SE) mode. (d) Freestanding triboelectric-layer (FT) mode.

contact, the charge transfers between their contact surface for the different competence of electrons gaining and losing [42]. Then the two plates form a parallel-plate capacitor and the induced charge on metal layers will transfer through external load when the plates separate along the vertical direction. In this mode, the wind is supplied to induce the contact and separation between the plates. A light-weight plate is easy to blow up but the output performance needs to be considered. The merit is that there is an inverse proportion between capacitor value and distance. It means that the value of a parallel-plate capacitor varies sharply when the distance between two plates changes by a tiny amount. In this case, a nearly maximum high output voltage can be reached within a limited separation distance.

Fig. 3b shows the LS mode TENG. The basic structure is similar to CS mode in that two opposite plates consisting of different dielectric materials adhered to metal electrodes, respectively. And the surfaces of dielectric materials also keep dissimilar carriers. The difference is that the plates have a relative movement along the horizontal direction. In LS mode, the electrodes contact each other and have a relative movement, which will cause undesirable friction. This kind of resistant friction is unsuitable for tiny energy collection, such as breeze wind. As a result, the LS mode structure TENG is seldom found in wind energy harvesting applications.

Fig. 3c shows the SE mode TENG. The uniqueness of this mode is that it has only one electrode with ground as the other common electrode. The TENG will output an alternating current signal as the dielectric layer separates and contacts with the ground-connected layer. For SE mode, the output performance is limited by the electrostatic shield effect with maximum charge transfer efficiency only 50 % [38]. Besides, since one of the electrodes is connected to the ground directly, the output signal will be affected easily if the external circuit is not filtered well.

FT mode TENG is similar to the LS mode, and the difference between them is that the electrodes of FT mode TENG are fixed (Fig. 3d). The dielectric material with carriers floats on plates and induces electricity between adjacent electrodes when moving. Theoretically, the FT mode with no friction is the best structure for energy harvesting. However, in practical application, the surface charge density of the dielectric layer will decrease with time. The dielectric layer usually has a very light contact with the fixed electrode. It will not only supplement the charge density but also improve the output performance. The closer the gap between the dielectric and the electrode, the more charges will be induced from the electrodes.

3. Structural design of the wind-TENG

Initially, wind-TENGs were designed to harvest wind energy at speeds of 5–10 m/s, and even higher [23,29,43]. However, to increase the energy-harvesting capacity of wind-TENGs, researchers have increasingly focused on designs that operate effectively at lower start-up wind speeds. As illustrated in Fig. 4a, the number of studies testing TENGs under lower wind speeds has gradually increased since 2017 [44]. For the practicability of wind-TENGs, however, structural improvements are needed to further reduce start-up wind speeds and enhance output performance. According to the evaluation of global wind power research conducted by Archer et al. [45], the average wind speed over land is 3.28 m/s, which is lower than that of a gentle breeze. This highlights the importance of achieving a lower start-up wind speed, especially since many regions experience consistently low wind speeds. Taking China's mean annual wind speed distribution as an example (Fig. 4b), around two-thirds of the mainland region has a mean annual wind speed below 3 m/s. If the start-up wind speed of a wind-TENG exceeds 3 m/s, the device would be inoperative for most of the time in these regions, rendering it ineffective and impractical for widespread deployment.

Therefore, based on the annual wind speed distribution mentioned above, we categorized the studies of nanogenerators on structural design into three types: wind-TENG with low start-up wind speed (below 3 m/s), wind-TENG with high start-up wind speed (above 3 m/s), and hybrid wind-TENG-EMG.

3.1. Wind-TENG with low start-up wind speed

3.1.1. Vibration structure wind-TENG

As for the vibration-based structural design, one notable advantage is its ability to accommodate a wide range of energy input directions. As shown in Fig. 5, the CS mode is particularly favored because vibrations naturally facilitate contact and separation inside the device. Ko et al. [46] designed a self-suspended shell-based wind-TENG (Fig. 5a) with an exceptionally low start-up wind speed of 0.3 m/s. The electrical output in this design is generated by irregular contact between the shell and a rigid column. Zhang et al. [47] proposed a CS mode TENG by utilizing a mass block and springs structure, where wind flow around the mass block induces vortex shedding, causing the mass to vibrate and drive the contact-separation action of the TENG (Fig. 5b). Another representative CS mode TENG design is based on a flapping structure. For example,

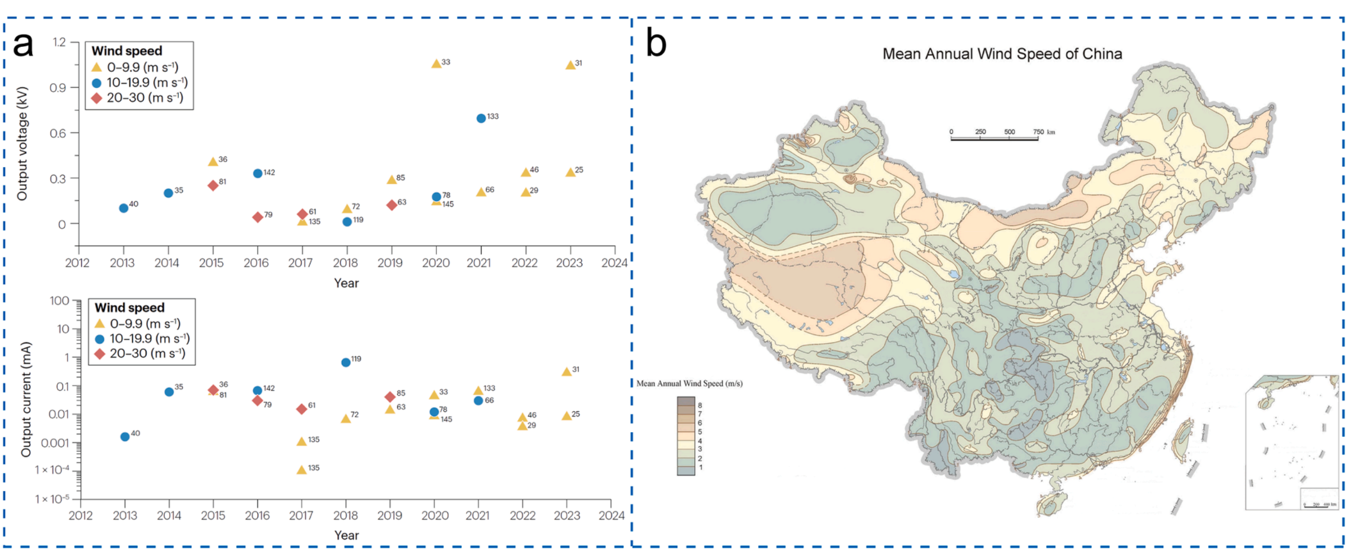

Fig. 4. (a) Performance evolution over the time [44]. (b) The mean annual wind speed distribution in China in 2019.
(a) Reproduced with permission.

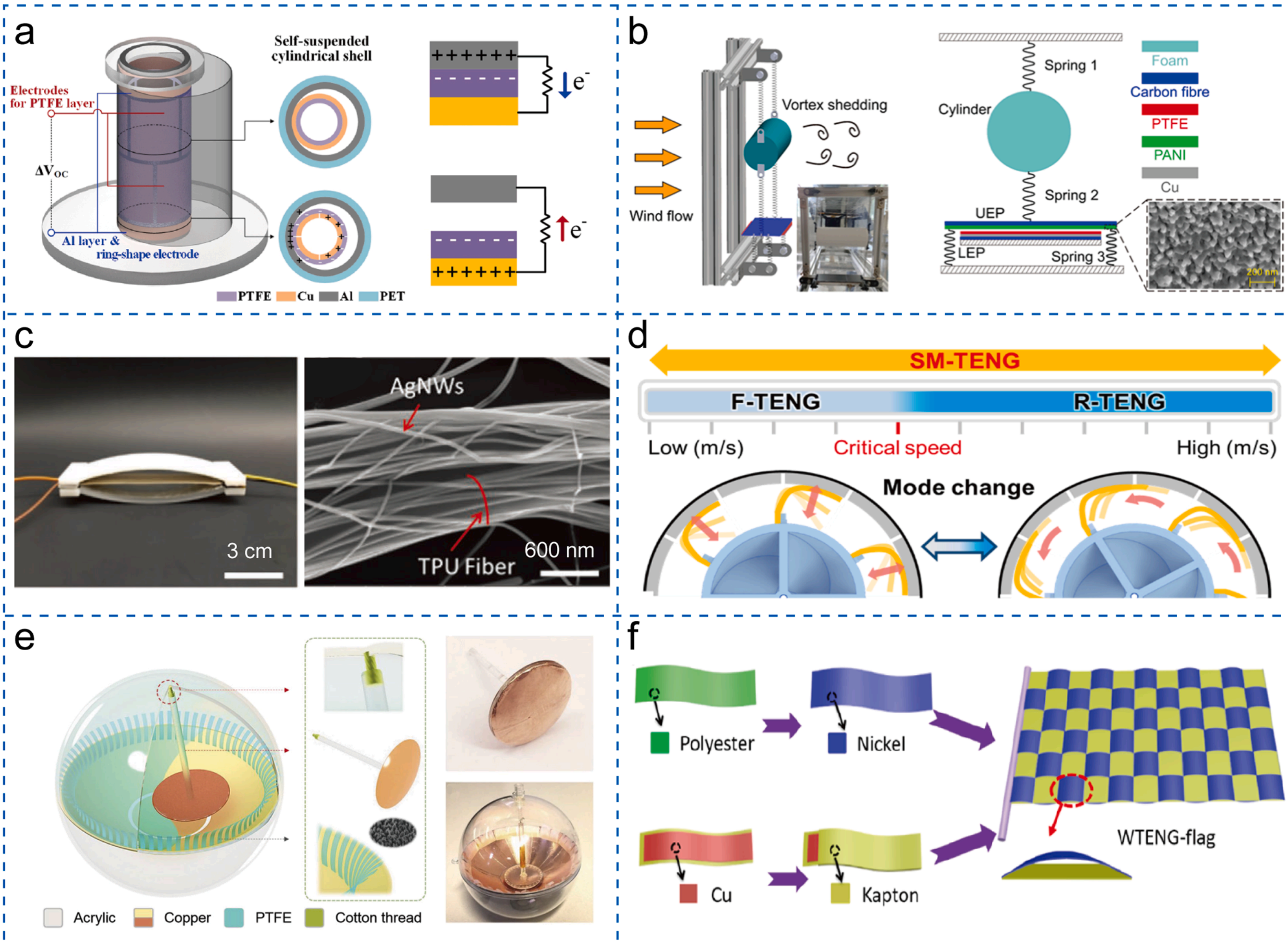

Fig. 5. Wind-TENG induced by vibration structure with low start-up wind speed. (a) Schematic diagram of self-suspended shell-based TENG [46]. (b) CS mode TENG with a mass block and springs structure [47]. (c) Schematic of gentle CS mode wind-driven TENG [49]. (d) Spontaneous working mode changeable TENG [50]. (e) Schematic illustration of pendulum-inspired TENG [51]. (f) Schematic illustration of the fabrication of flag-like TENG (WTENG-flag) [52]. Reproduced with permission.

Tian et al. [48] proposed a dual auxiliary beam galloping TENG with fluorinated ethylene propylene (FEP) and polyaniline (PANI). As the middle plate vibrates, it alternately contacts the adjacent plates, generating an open-circuit voltage of approximately 100 V at a start-up wind speed of 1.7 m/s. Further, Ren et al. [49] proposed a gentle CS mode wind-driven TENG whose electrifying material is composited by thermoplastic urethane (TPU) and silver nanowire (Fig. 5c). The fabricated device exhibits a extreme low start-up wind speed of 0.7 m/s due to the superelasticity of the composited material.

In addition to CS mode vibration TENGs, Cho et al. [50] conceived a spontaneous working mode changeable TENG based on erratic wind conditions (Fig. 5d). The device can operate in SE mode at a start-up wind speed of 2.5 m/s and translate to FT mode when the wind speed exceeds 5 m/s. Unfortunately, as previously mentioned, the output of the SE mode structure is limited, and this kind of TENG can only generate an output of 1.5 V at a low wind speed of 2.5 m/s.

Additionally, some structure designs are inspired by daily life. For example, inspired by the swing tree in windy, Lin et al. [51] developed a pendulum structure wind-TENG based on the FT mode (Fig. 5e). A typical application scenario involves hanging the TENG on a tree, where the unstable pendulum, coated with copper foil, swings and interacts with strips at the edges, thereby generating electrical output. Similarly, Zhao et al. [52] designed an FT mode flag-type TENG for harvesting high-altitude wind energy (Fig. 5f). Nickel-coated polyester textiles and copper-coated Kapton films were woven the flag as triboelectric materials. When the wind blows, the flag flutters, causing contact and separation between the woven textiles, which generates electrical output.

3.1.2. Rotation structure wind-TENG

In the case of rotation structure TENGs, windmills or blades usually serve as the basic component of the device. Both vertical and horizontal blades are used in structural design. Vertical blades are capable of capturing wind energy from any direction, while horizontal blades can only harvest energy from a single direction. For horizontal designs, Gulahmadov et al. [53] exhibited a unique TENG structure based on the CS mode (Fig. 6a,b). They used a crank to convert the rotation into a linear reciprocating motion, and a zigzag origami structure was designed to multiply TENG's pair to improve the output performance. It is important to carefully design the gap distance in CS mode TENGs, as insufficient distance can cause collisions between the moving and fixed plates, wasting wind energy.

Different from the vibration structure, the most popular rotation structure design is based on FT mode (Fig. 6) due to its rotational functionality and low friction resistance. Another notable horizontal windmill design, shown in Figs. 6c and 6d, was developed by Fu et al. [54] featuring a low-friction structure with rollers, achieving a start-up wind speed of 2 m/s. The planetary rolling structure, which converts sliding friction into rolling friction by contacting the electrodes, reduces

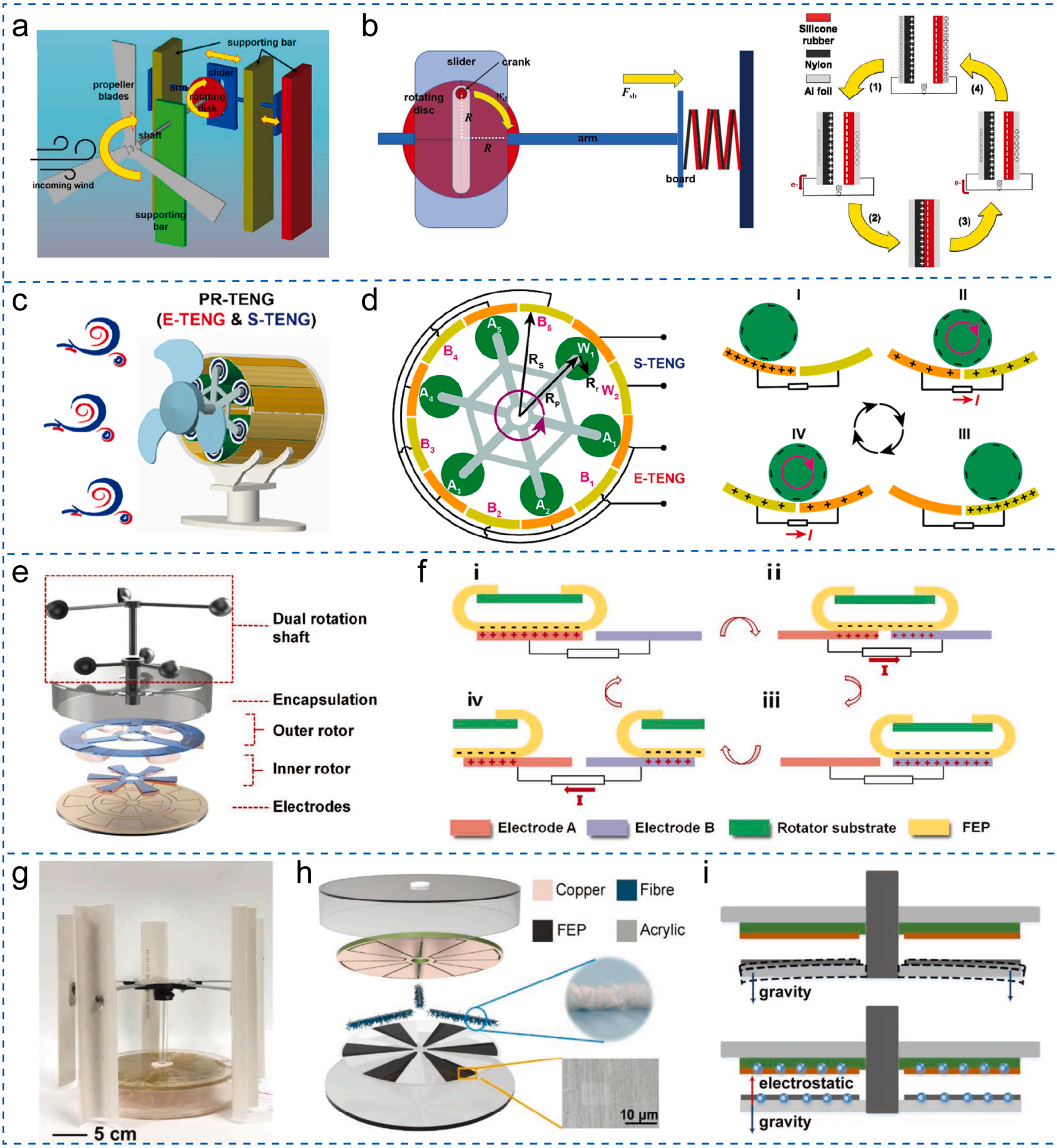

Fig. 6. Wind-TENG induced by rotation structure with low start-up wind speed. (a,b) Illustration (a) and the operation principle (b) of the CS mode wind-TENG [53]. (c,d) Framework for horizontal wind-TENG (c) and schematic diagram showing the planetary rolling structure of wind-TENG based on FT mode (d) [55]. (e,f) A double rotors structure design of wind-TENG (e) and its typical output performance (f) [56]. (g–i) Photograph of vertical wind-TENG (g) and illustration of the detailed structure (h) and a novel inverse structure design of wind-TENG (i) [21].
Reproduced with permission.

friction resistance and improves output performance. In addition, a modified structure that adds a dielectric membrane between the electrodes and rollers demonstrated enhanced durability, withstanding continuous operation for 6.4 million cycles [55].

For vertical windmill design, considering that the rotor with a longer force arm has a larger torque, it needs more energy to power on. Yong et al. [56] proposed a double-rotor design (Fig. 6e,f), where the shorter rotor collects low-speed wind energy and the longer rotor captures higher-speed wind energy. This expands energy harvesting over a broad-band wind speed range of 2.2–16 m/s. Additionally, Liu et al. [21] designed the wind-TENG with a start-up wind speed of about 1 m/s (Fig. 6g). The structure consists of a slim acrylic disc rotor covered with FEP and a printed circuit board stator. Ultrafine fiber stuck at the electrode gap and FEP served as the triboelectric materials (Fig. 6h). The slim rotor and fiber materials minimize frictional resistance to nearly zero. The novel design of this work involves an inverse structure where the rotor is positioned beneath the stator (Fig. 6i), using the rotor's weight to counterbalance the electrostatic force and prevent rotation deadlock.

To date, the primary structural designs achieving lower start-up wind speeds are based on CS and FT modes. The lowest recorded start-up wind speed is below 1 m/s, with a maximum transfer charge quantity of less than 200 nC and a maximum short-circuit current of less than 4 μA. Table 1 summarizes the working modes, triboelectric materials, peak-to-peak open-circuit voltage (V_{pp}), peak-to-peak short-current (I_{pp}), and charge transfer quantity of wind-TENGs operating at start-up wind speeds of approximately 2 m/s.

3.2. Wind-TENG with high start-up wind speed

Although some structures have a minimum start-up wind speed higher than 3 m/s, they still exhibit impressive performance metrics. For example, Li et al. [64] designed a breeze-driven TENG (BD-TENG) with a start-up wind speed of 3.3 m/s, as shown in Fig. 7a. Despite this, the device demonstrated commendable output at a wind speed of 4 m/s, with an open-circuit voltage of 330 V, short-circuit current of 7 μA, and transferred charge quantity of 137 nC. Since Yang et al. introduced the first wind-TENG structure in 2013 [17], Lin et al. [65] integrated several similar devices together to improve the output performance. Further, Zhao et al. [66] adapted this design (Fig. 7b), substituting the material with a composite film to improve output performance (Fig. 7c). At a wind speed of 6 m/s, the TENG utilizing the $0.94(Bi_{0.5}Na_{0.5})TiO_3$ - $0.06Ba(Zr_{0.25}Ti_{0.75})O_3$/polyvinylidenefluoride (BNT - BZT/PVDF) composite film reached the V_{pp} of about 200 V and I_{pp} of 20 μA, respectively.

Moreover, Lee et al. [67] developed a stackable disk-shaped TENG designed to harvest omnidirectional wind (Fig. 7d). Wind guides were used as inlets and outlets, converting the wind into vortex flow (Fig. 7e, f). Polytetrafluoroethylene (PTFE) spheres were blown to collide the electrodes, generating an electrical output. Although the start-up wind speed was relatively high (6.5 m/s) and the output performance was limited (maximum rectified voltage of 18 V), the structure provides valuable insights for future designs. Mu et al. [68] addressed the challenge of enhancing durability using a soft contact approach, balancing the trade-off between soft contact and large charge density. They devised a novel blade soft contact TENG with shielded electrodes on the rotor, while charge accumulation and dissipation occurred on the stator (Fig. 7g,h). This TENG achieved a charge density of 328 $\mu C/m^2$. At a wind speed of 5.5 m/s, the output charge, I_{pp}, and V_{pp} were approximately 1.7 μC, 400 μA, and 2500 V. The device can successfully power 3840 green LEDs or 80 parallel hygrothermometers simultaneously (Fig. 7i). Table 2 summarizes the structure mode, materials, V_{pp}, I_{pp}, and charge transfer quantity of wind-TENGs operating at wind speeds ranging from 5.5 m/s to 6.5 m/s.

Table 1
The output performance of wind-TENG with lower start-up wind speed.

Working mode	Materials	V_{pp} (V)	I_{pp} (μA)	Qsc (nC)	Ref.
SE	Kapton, Aluminum	1.5	< 1	–	* [50]
CS	Silicone rubber, Nylon	12	1.5	–	[53]
CS	Aluminum, PTFE	8	–	–	[46]
CS	FEP, Aluminum	300	12	200	[57]
CS	PTFE, steel	200	7	80	[58]
CS	PTFE, polyaniline	400	10	58	[47]
CS	FEP, Nylon	200	5	–	[59]
FT	Glass, Copper	15	0.5	–	[60]
FT	Glass, Copper	210	9	–	[54]
FT	Fur, FEP	–	6	170	[61]
FT	PTFE, Cotton	50	0.5	–	[51]
FT	FEP, mop Fiber	2500	–	300	[21]
FT	FEP, Copper	3	0.5	–	[62]
FT	FEP, silver nanowires	150	12	–	[49]
FT	Polyimide, Aluminum	72	< 8	–	[63]
FT	FEP, polyaniline	52	8	–	[48]
FT	FEP, copper	75	4	60	[56]

* The data are tested under 2.5 m/s.

3.3. Hybrid wind-TENG-EMG

As mentioned above, wind-EMGs can not work efficiently at a low frequency. By combining TENGs with EMGs to create hybrid wind-TENG-EMG systems, the wind speed response range can be expanded, resulting in improved output across a broader operational frequency bandwidth. In this section, we will summarize recent advancements in the development of hybrid wind-TENG-EMG systems.

Hybrid wind-TENG-EMGs, like EMG and TENG, are also commonly designed based on rotation structure [70]. Rahman et al. [71] combined the TENG with EMG by 3D printed technology, exhibiting a start-up wind speed of 3 m/s (Fig. 8a). The rotating windmill drove the blades to contact edge electrodes and the magnets to produce a changeable magnet field, making the TENG and EMG operate simultaneously. Rahman et al. [72] and Luo et al. [73] devised different low start-up wind speed hybrid generators respectively, giving considerations to the durability enhancement. Rahman implemented a magnet in stationary TENG, and the alternating attraction and repellency of the rotating magnet pushed the TENG to operate at CS mode (Fig. 8b). This contactless triggering-based generator minimized the start-up wind speed to 1 m/s and possessed an ultra-robust character meanwhile. Luo designed an automatic switching structure by using a gear train and cam switch (Fig. 8c), achieving a stable mode transition between contact and non-contact modes. The non-contact mode effectively reduced the start-up wind speed to 2 m/s and significantly prolonged the lifetime of TENG. At the same time, Yong et al. [74] also designed a self-adaptive hybrid wind-TENG with a comparable start-up wind speed of 2 m/s but performs an efficient energy collection of 41.05 W/m^3. Moreover, there are also some other commendable structures. Similar to Zhao's [52] work, Ye et al. [75] added an additional EMG on the flagstaff (Fig. 8d), expanding the wind speed response range. And similar to Gulahmadov's work, Fan et al. [76] devised an elliptical-shaped structure to convert the rotation to linear reciprocating motion (Fig. 8e). The start-up wind speed is 4 m/s, and the maximum output power of TENG and EMG are 0.36 mW and 18.6 mW at the wind speed of 9 m/s, respectively.

4. Power management circuits for enhanced energy storage

Notably, the output of TENG is typically characterized by low-frequency pulsed energy with high voltage and low current, making it inadequate to directly power the terminal devices. A practical approach for self-powered system realization is to save the energy into a capacitor until the energy is sufficient to power the load [77], exposing the crucial importance of energy storage. The initial energy storage strategy utilizes a rectifier bridge transmitting the TENG's energy to the capacitor. However, the energy-storage efficiency has been constrained due to the huge impedance mismatch between the TENG and the storage component. To overcome this limitation, the integration of power management circuits is crucial for the practical application of self-powered systems. One strategy involves the design of switching capacitor circuits to efficiently extract energy from TENGs to storage capacitors. Another approach focuses on accelerating the charging process by employing a switch to LC resonant buck circuit. In this section, we will summarize recent advancements in the development of these two power management strategies for improving the energy storage efficiency of self-powered systems based on wind-TENGs.

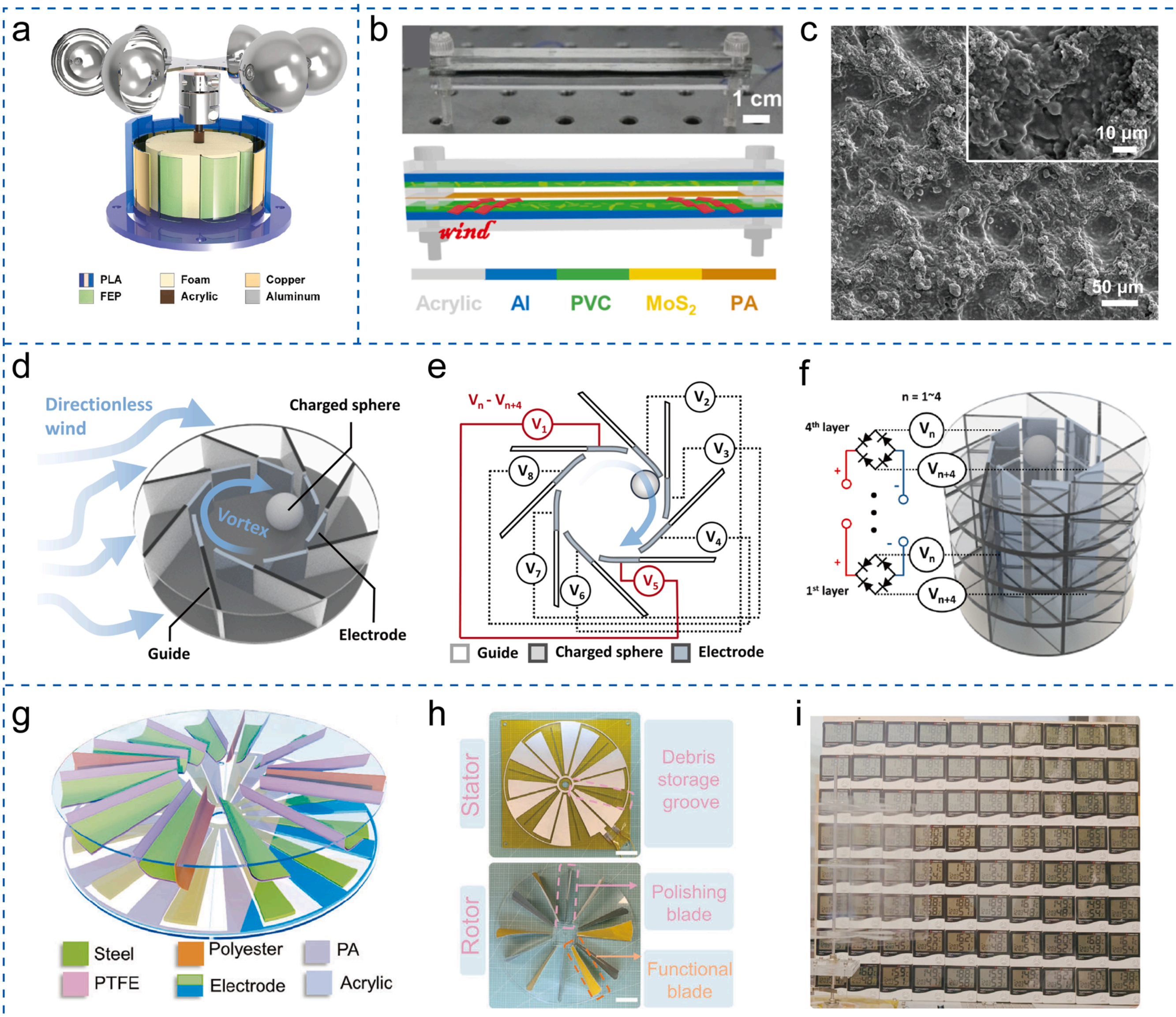

Fig. 7. Wind-TENG with higher start-up wind speed. (a) Illustration of the BD-TENG structure [64]. (b,c) A schematic diagram of the TENG (bottom) and photograph (top) (b) and an SEM image of the composite film (c) [66]. (d–f) Schematic structure of wind-TENG (d) and circuit diagram of the freestanding mode and measurement method (e) schematic of the four-layer-stackable wind-TENG (f) [67]. (g–i) 3D structure diagram of the TENG (g), photograph of stator and rotor (h), and the enlarged optical picture of 80 hygrothemometers working simultaneously (i) [68].
Reproduced with permission.

Table 2
The output performance of wind-TENG with higher start-up wind speed.

Structure	Materials	V_{pp} (V)	I_{pp} (μA)	Qsc (nC)	Ref.
FT	PTFE, Aluminum	5	–	–	[67]
FT	FEP, copper	315	13	–	[64]
FT	Polyester, PTFE	2500	400	1500	[68]
FT	Polyamide, composite	200	10	–	[66]
FT	Polyamide, composite	150	20	–	[69]

4.1. Switching capacitor buck converter

Ghaffarinejad et al. [27] proposed a conditioning circuit with exponential enhancement of output energy based on Bennet's doubler principle (Fig. 9a). The study provided a theoretical analysis of the charge-voltage evolution dynamics within Bennet's circuit. And the results demonstrated that Bennet's circuit could achieve an output several orders of magnitude higher compared to conventional full-wave and half-wave circuits. Liang et al. [78] proposed a MOSFET-based charge excitation circuit (Fig. 9b), where one P-type MOSFET and two N-type MOSFET were utilized to control energy charging and release. Initially, two small parallel capacitors are charged to the same voltage *U* and charge quantity *Q*, assuming the capacitors are equal. When the capacitors are switched to a series connection, the output voltage doubles.

Xu et al. [79] and Liu et al. [80] proposed a charge excitation method by exploiting a pump TENG to enhance the output performance of the main the TENG. In Fig. 9c, the rectified charges from the pump TENG were injected onto the surface of the main TENG, leading to an enhanced output due to increased charge density. Building on this concept, Chung et al. [81] applied this strategy to boost the performance of a fluttering TENG (Fig. 9d). In this design, unidirectional primary wind flows through the main TENG, while residual ambient wind flows through a charge-supplying TENG. The charges from the supplying TENG augment the main TENG's output, resulting in enhanced performance.

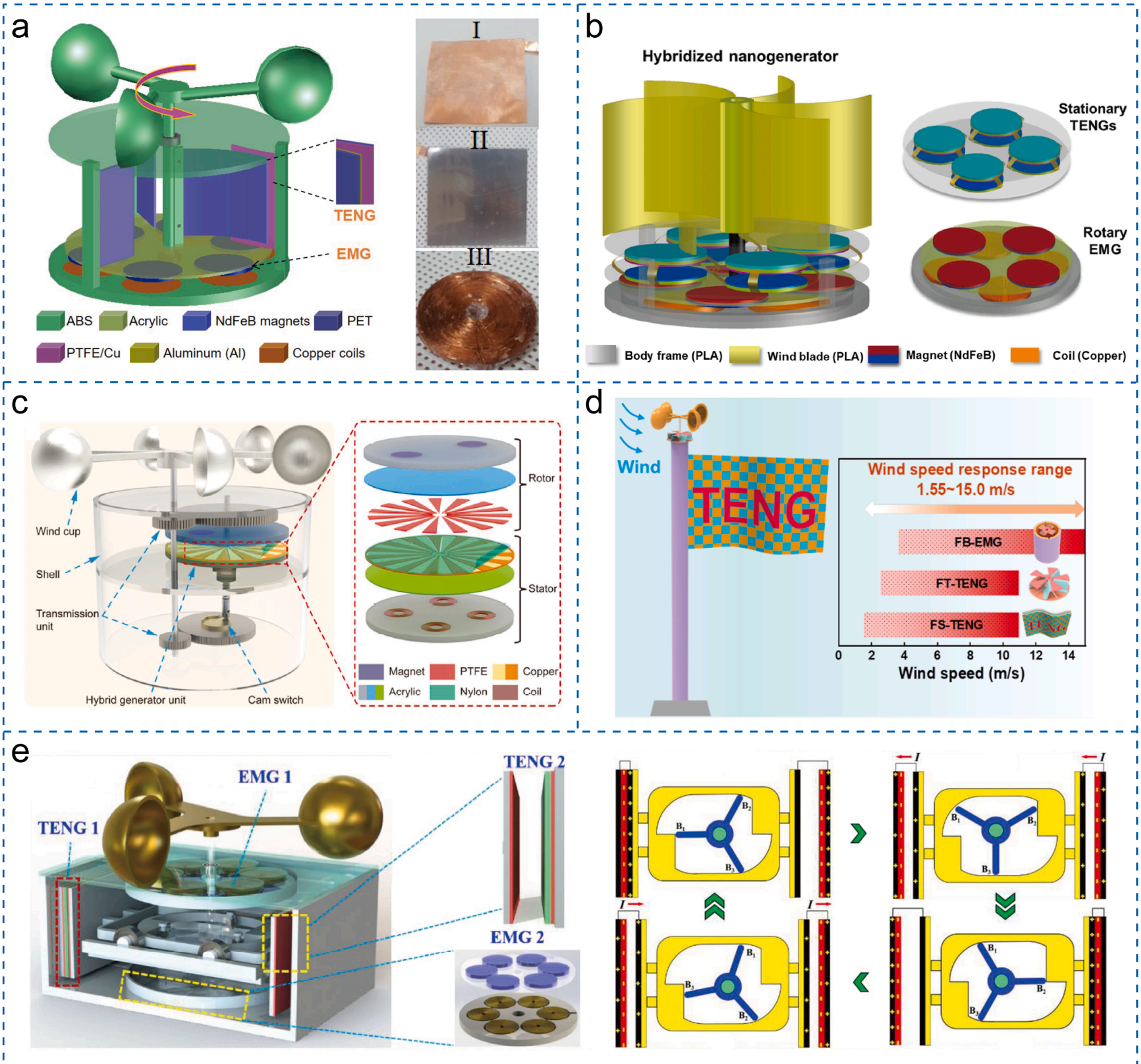

Fig. 8. Wind-TENG and EMG hybrid structures with higher start-up wind speeds. (a) Schematic design of the natural wind-TENG hybrid nanogenerator [71]. (b) Schematic of a contactless mode triggering-based ultra-robust hybridized nanogenerator that mainly consists of an array of four stationary contact-separation mode-based TENG and a rotating EMG [72]. (c) The whole structure of the hybrid device [73]. (d) The combination of wind-TENG and wind-EMG [75]. (e) Schematic of hybrid nanogenerator structure and working principle [76].
Reproduced with permission.

4.2. LC resonant buck converter

Charging technology can be clarified to Constant Voltage (CV) mode and Constant Current (CC) mode [82,83]. CV mode charging circuits, such as full bridge circuits [15,84] are relatively simple and have garnered significant attention in the early stages of TENG energy harvesting research. These circuits feature a high initial charging current; however, as the capacitor's voltage increases, the charging current decreases, leading to lower charging efficiency. To address the need for higher charging speeds and efficiency, recent studies have focused on CC mode charging circuits, which typically consist of a switch and a resonant circuit. The switch regulates power release to the resonant circuit, while the resonant circuit, usually a buck circuit with an inductor and a capacitor connected in series, reduces high voltage, maintains a constant current, and stores the harvested energy.

For switch realization, Qin et al. [85] and Zhang et al. [86] proposed some delightful designs to let the TENG discharge at the maximum voltage moment realizing a switch function, but this approach needs an individual structural design for each unique application. Besides this, another two approaches are commonly employed: using discrete components, such as MOSFETs and silicon-controlled rectifiers (SCRs), or directly designing an electronic switch. In the discrete components approach, Xi et al. [87] designed a universal power management module in 2017, which was later widely applied in wind-TENGs. The switching circuit consists of a MOSFET and a comparator, with the comparator outputting a pulse to trigger the MOSFET when the input voltage exceeds the reference voltage. When the input voltage falls below the reference voltage, the MOSFET is turned off. Due to TENG's sharp

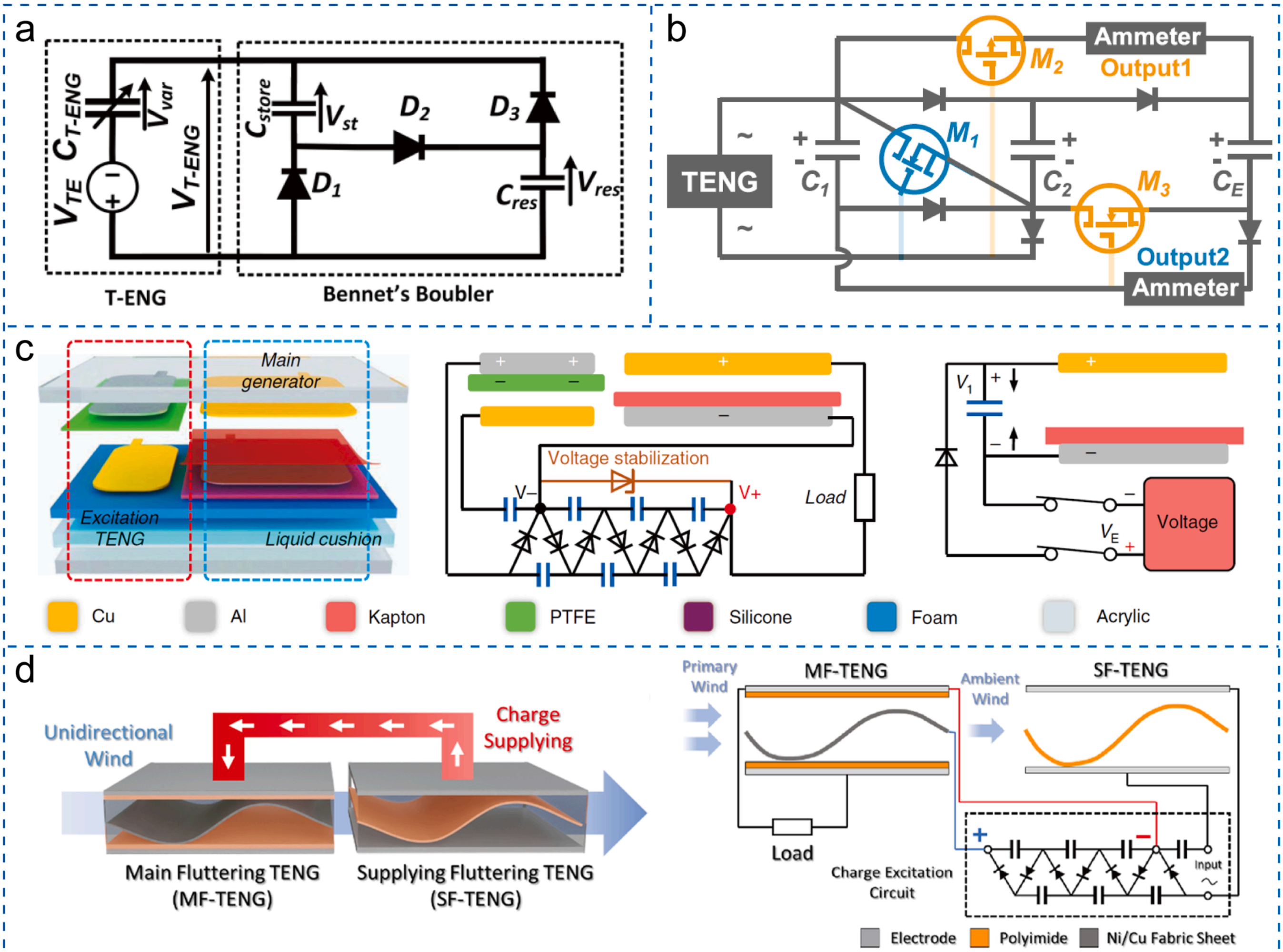

Fig. 9. Circuit design strategy for enhancing the output energy of wind-TENG (T-ENG). (a) Illustration of the Bennet's doubler circuit [27]. (b) Schematic of the MOSFET-based power management circuit [78]. (c) The systematical electric circuit scheme of TENG [80]. (d) The systematical design of wind-TENG derived from the charge pump structure [81].
Reproduced with permission.

output, the MOSFET's opening time is narrow, in the range of microseconds, allowing a high instantaneous voltage to reach the buck circuit. The inductor transfers the instantaneous electricity to magnetic field energy, which then releases and maintains a constant current, leading to a fast energy saving in the storage capacitor. Similarly, in 2020, Harmon et al. [28] designed another CC mode power management circuit by using a silicon-controlled rectifier (SCR), a Zener diode, and a buck circuit. In this circuit, the Zener diode is used to trigger SCR for power release when the capacitor C_{in}'s voltage exceeds the Zener diode's breakdown voltage plus the capacitor C_{out}'s voltage. The energy is then directed to the buck circuit, maintaining a constant current through resonance between the inductor and capacitor, achieving an overall energy conversion efficiency of 84.3 %. The advances in discrete component utilization have enabled the circuits to be customized for improved adaptation to TENG systems. In 2022, Liu et al. [21] extended Harmon's work by adding a part of the under voltage lock output (UVLO) circuit between the capacitor C_{store} and load (Fig. 10c). Using the LTC3588 chip, the UVLO circuit can automatically output the energy once the voltage of C_{store} reaches a desired value, marking significant progress toward a totally self-powered system. Other works also demonstrate the effectiveness of this power management circuit design [88–90].

For the electric switch designing approach, Wang et al. [91] and Luo et al. [73] replaced the SCR with a spark switch (Fig. 10d) and a ceramic gas discharge (CGD) tube (Fig. 10e), respectively. These circuits are activated when the voltage of the capacitor C_{in} exceeds the breakdown threshold of the spark switch/CGD tube. Furthermore, Yan et al. [34] proposed a flexible film-discharge-switch (FDS) based on the electrostatic breakdown (Fig. 10f), compatible with four different TENG modes. The FDS is fabricated like a parallel-plate capacitor with an additional PTFE insulation layer between the metal scraps. This flexible and lightweight (0.025 g) device offers customization of conductive voltage for the rear buck circuit by adjusting the insulation layer's thickness. The typical characteristic of the FDS shows a 1.85 kV breakdown voltage with an insulation thickness of 400 μm at around 40 % humidity. Moreover, the FDS exhibits a high energy-transfer efficiency (86.7 %) and excellent durability, withstanding up to 1.25 million discharge cycles.

5. Applications of wind-TENG

As the structures and power management circuit of the wind-TENG develops, practical applications of self-powered sensors and systems come up in various areas, for example, agriculture, transportation, wireless environmental sensing, and so on [92]. A detailed introduction to these applications will be given in this section.

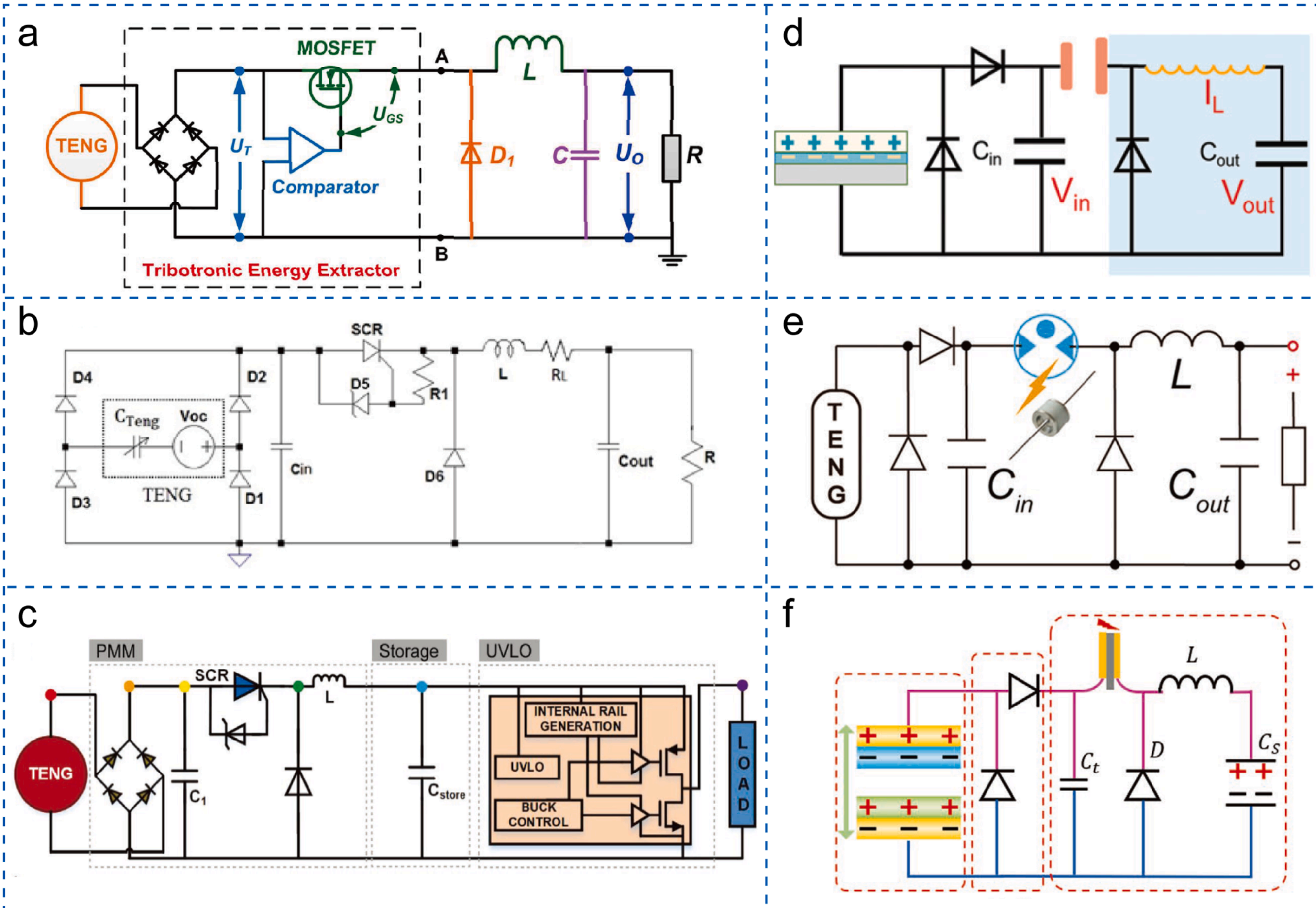

Fig. 10. Power management circuit designed for improving the charging speed. (a) The schematic circuit diagram of AC-DC buck conversion by coupling TENG, rectifier, comparator circuit, and DC-DC buck converter [87]. (b) The complete circuit diagram of the SCR-based power management circuit [28]. (c) The topology of a self-starting circuit design with a power management circuit, storage capacitor, and under voltage lock output circuit [21]. (d–f) Schematic design of the power management circuit with spark switch [91] (d), ceramic gas discharge tube [73] (e), and fabricated switch [34] (f).
Reproduced with permission.

5.1. Applications in agriculture area

Agricultural activities, such as chemical fertilization, often cause environmental damage. As an eco-friendly technology, wind-TENG exhibits significant potential for promoting agricultural sustainability. Due to the high voltage of TENG, they can not only enhance seed germination but also stimulate seedling growth. Li et al. [93] designed a wind-TENG that generates a 6 kV alternating voltage at a wind speed of 5.9 m/s (Fig. 11a). When the rectified voltage was applied to pea seeds, experiments showed that germination speed and yield increased by approximately 26.3 % and 17.9 % (Fig. 11b), respectively, under an electric field of 2 kV/cm. Additionally, the electric field promoted seedling growth in both height and weight, likely due to electric field-induced physiological activities, and similar works also demonstrate the high voltage effectiveness of crops growth promotion [30]. Since TENGs can catalyze the synthesis of compounds such as NO_x and ammonia, these compounds may contribute to seedling growth [94]. For instance, Wang et al. [95] developed a lightweight wind-TENG for self-powered electrocatalytic nitrate-to-ammonia conversion (Fig. 11c). With a low start-up wind speed (3 m/s), the TENG charged and discharged a 0.01 F capacitor, achieving a high NH_3 yield of 11.48 μg/cm^2/h. This work demonstrates a system coupling electrocatalysis with natural energy harvesting for NH_3 synthesis, offering an environmentally friendly method for chemical fertilizer production in agriculture.

Han et al. [61] conceived a smart farming system by combining a series of sub-level applications including a night direction display (Fig. 11d), a mosquito trap, self-powered soil moisture sensing, and temperature and humidity monitoring. Particularly, a UV lamp powered by the wind-TENG was used to trap the mosquitos (Fig. 11e), which could be extended to other insect trap applications without the need for harmful pesticides [96]. Additionally, Zhao et al. [66] demonstrated a water pH detection system by powering a commercial pH meter (Fig. 11f), Li et al. [64] powered a soil thermometer to monitor the soil temperature, while Jeon et al. [97] proposed a Wind-TENG driven water treatment system, all of which are critical applications for smart farming.

5.2. Applications in transportation area

Vehicles, as one of the most widely used transportation tools, require extensive information sensing. For instance, in the development of hydrogen-powered vehicles, detecting hydrogen leakage is crucial for safe driving. Jiang et al. [98] developed a self-powered hydrogen leakage sensor based on a windmill-like TENG (Fig. 12a). The TENG is mounted on the automobile's air intake window and converts airflow energy into power for the hydrogen sensor. The equivalent circuit is shown in Fig. 12b, where the resistance of the hydrogen sensor decreases with increasing gas concentration. This change in resistance affects the divided voltage on the resistance R_0, which is reflected in the brightness of the alarming LED_1.

For highway vehicle applications, Su et al. [99] designed a series of

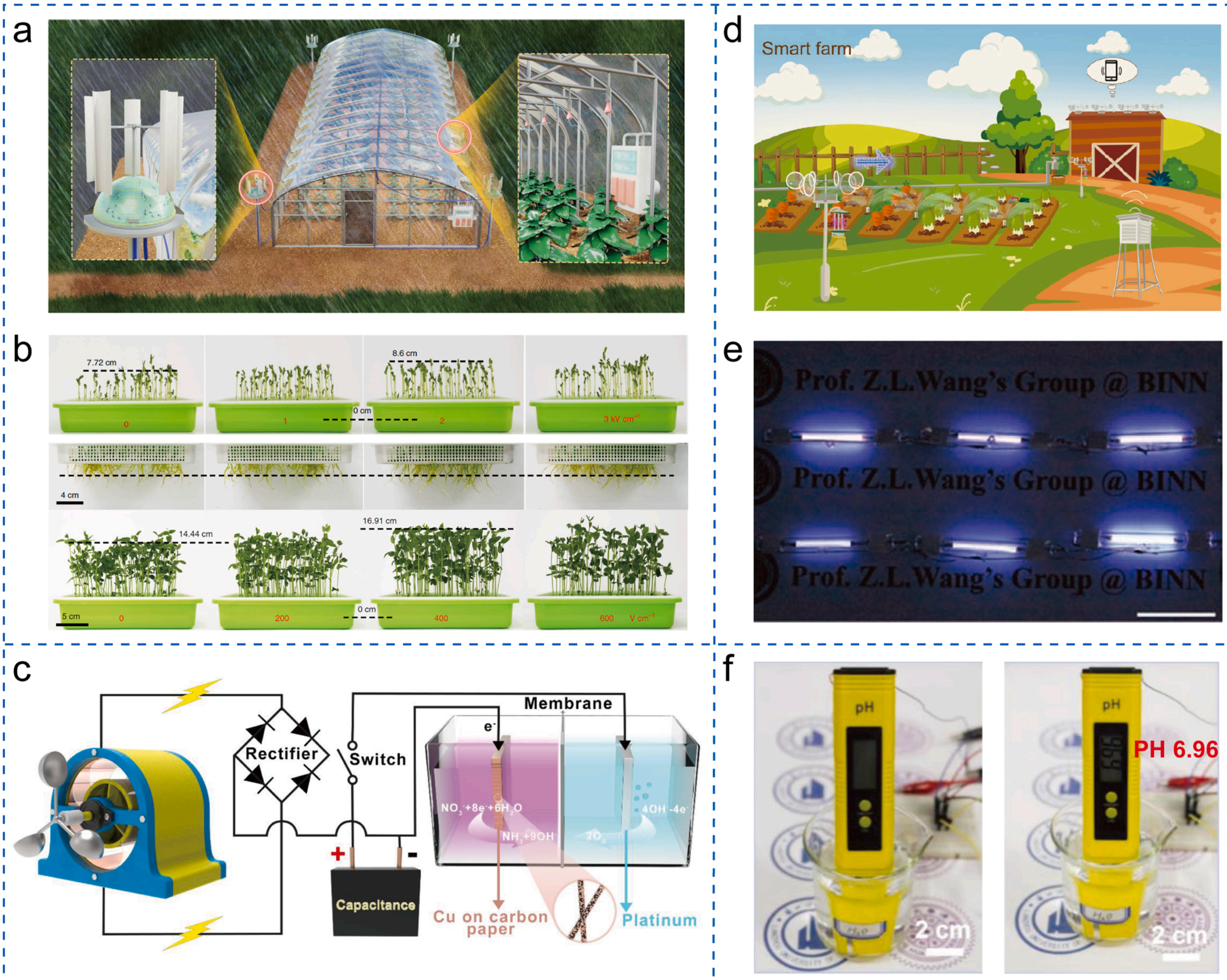

Fig. 11. IoT application of wind-TENG in agriculture area. (a,b) Application scenario of wind-TENG used for applying high voltage in the farm (a) and germination promoting result (b) [93]. (c) Schematic of the wind-TENG driven electrochemical nitrate reduction reaction to ammonia system [95]. (d,e) wind-TENG used in a smart farm (d) and used for powering a UV lamp powered by wind-TENG used for mosquito trapping (e) [61]. (f) Photograph of a wind-TENG powered commercial water pH meter [66].
Reproduced with permission.

wind-mill-like TENG sensing nodes aligned along the freeway (Fig. 12c). These nodes can be integrated with wireless sensors such as active RFID tags, which are powered by wind-TENGs. The tag could transmit signals like geological location, travel path, and car speed to the passing car. This system has potential applications in potential global positioning systems (GPS). What's more, the blades of the wind-TENG offer an anti-glare effect (Fig. 12d), improving lateral visibility for drivers by blocking incoming light. Further, Zhang et al. [100] conceived a more challenging application for self-powered high-speed railway sensors. They positioned a TENG near the track to recover wind energy generated by passing high-speed trains and power related sensing devices. Potential applications include railway bridge monitoring, track data monitoring (Fig. 12e), and railway meteorological monitoring, all critical to railway safety. The TENG features a double-layer design with an elastic rotator located between the stator (Fig. 12f). The TENG device can output a peak power of 29.1 mW at a wind speed of 20 m/s, which is well below 100 m/s wind speeds generated by high-speed trains.

What's more, apart from the wind-TENG used as an energy harvester, the wind-TENG is most frequently used as gas/wind speed sensor. In marine applications, Du et al. [101] proposed a self-powered and robust exhaust gas flow sensor based on a bearing type TENG (Fig. 12g). The sensor uses six steel balls and PTFE film as friction materials, with six additional PTFE balls to stabilize the rolling motion. The gas flow speed correlates linearly with the output signal frequency, and the device successfully monitors gas flow speed with a correlation coefficient greater than 0.998. The test result shows that the mean error between this device and a commercial sensor is only about 0.73 %.

5.3. Applications in environment monitoring

A series of self-powered environment monitoring sensors and systems have been developed to address pollution problems caused by fuel usage. By integrating monitoring applications with wireless technology, the range of environmental sensing can be greatly expanded. Early studies favored Bluetooth as the most popular choice. For self-powered sensor, typically, Zou et al. [102] developed a wind speed measurement system by converting the airflow-induced rotation speed into the wave numbers of the TENG signal (Fig. 13a). Simultaneously, the wind-TENG charges a supercapacitor and then powers the whole system, enabling real-time sampling and data transmission to a Bluetooth receiver. For environment monitoring systems, Liu et al. [103] designed a CO concentration sensing node to monitor the gas pipes for air quality

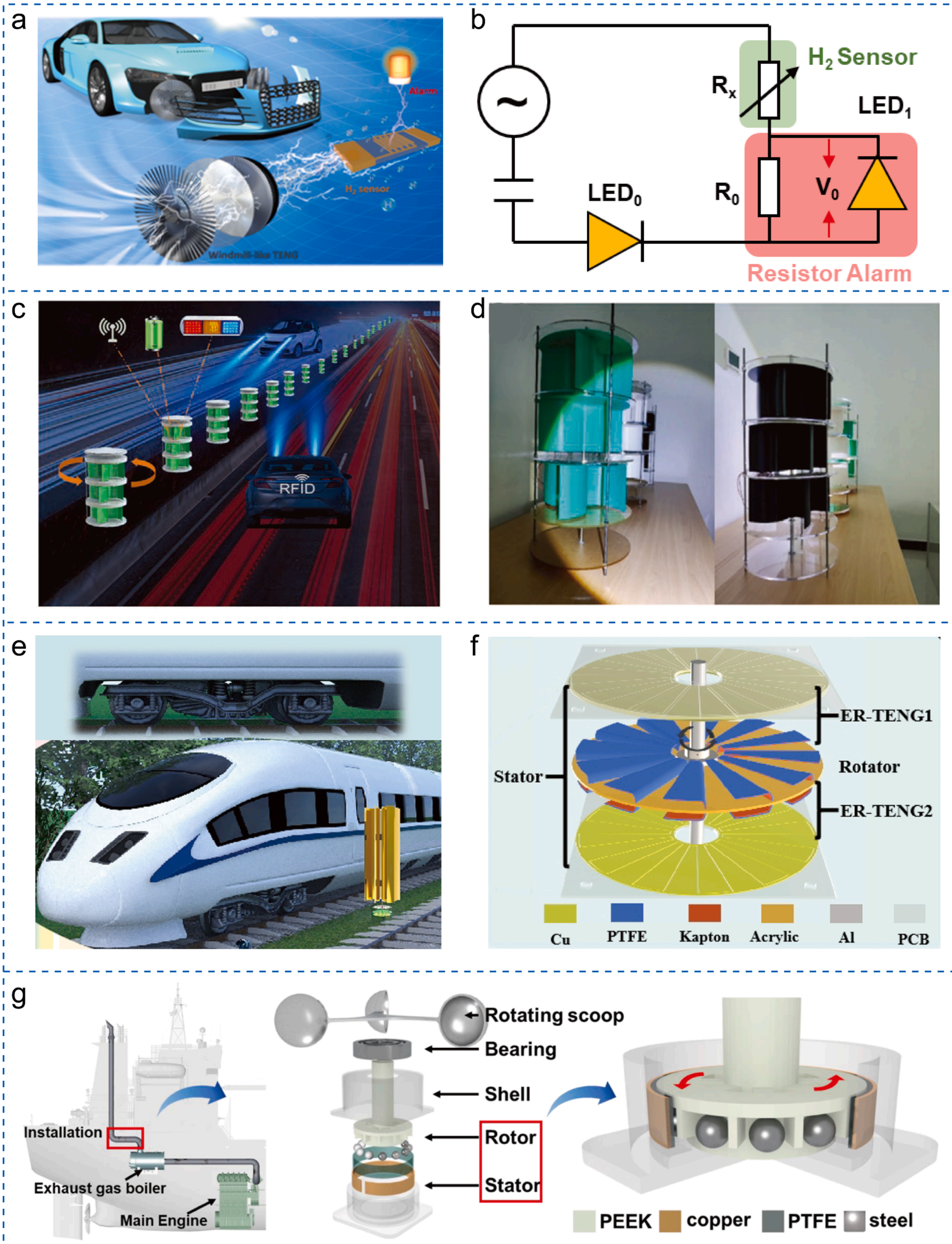

Fig. 12. IoT application of wind-TENG in transportation area. (a,b) Schematic diagram of the self-powered hydrogen leakage sensing system (a) and the equivalent circuit of the system (b) [98]. (c,d) The configuration of wind-TENG installed in the highway isolation belt (c) and anti-glare effect of wind-TENG under simulated high beam illumination (d) [99]. (e,f) Application scenario of railway track information detection (e) and the schematic representation of the structure of double-layer TENG (f) [100]. (g) Schematic scenario and structure of the bearing type TENG [101].
Reproduced with permission.

protection. A 7.2 mF capacitor can be charged to 3.6 V within 1000 s at a wind speed of 4.5 m/s, allowing the system to transmit data via Bluetooth. Sou et al. [104] also proposed a Bluetooth offshore environment monitoring system based on a Savonius turbine Wind-TENG operating on the sea. Under a wind speed of 7.2 m/s, a message can be tracked through Bluetooth every 20 s. The advancement of low-power Bluetooth technology has directly facilitated the development of these self-powered environmental applications.

Further, Li et al. [105] designed a self-powered forest ambient monitoring microsystem by using Zigbee (Fig. 13b), another mainstream

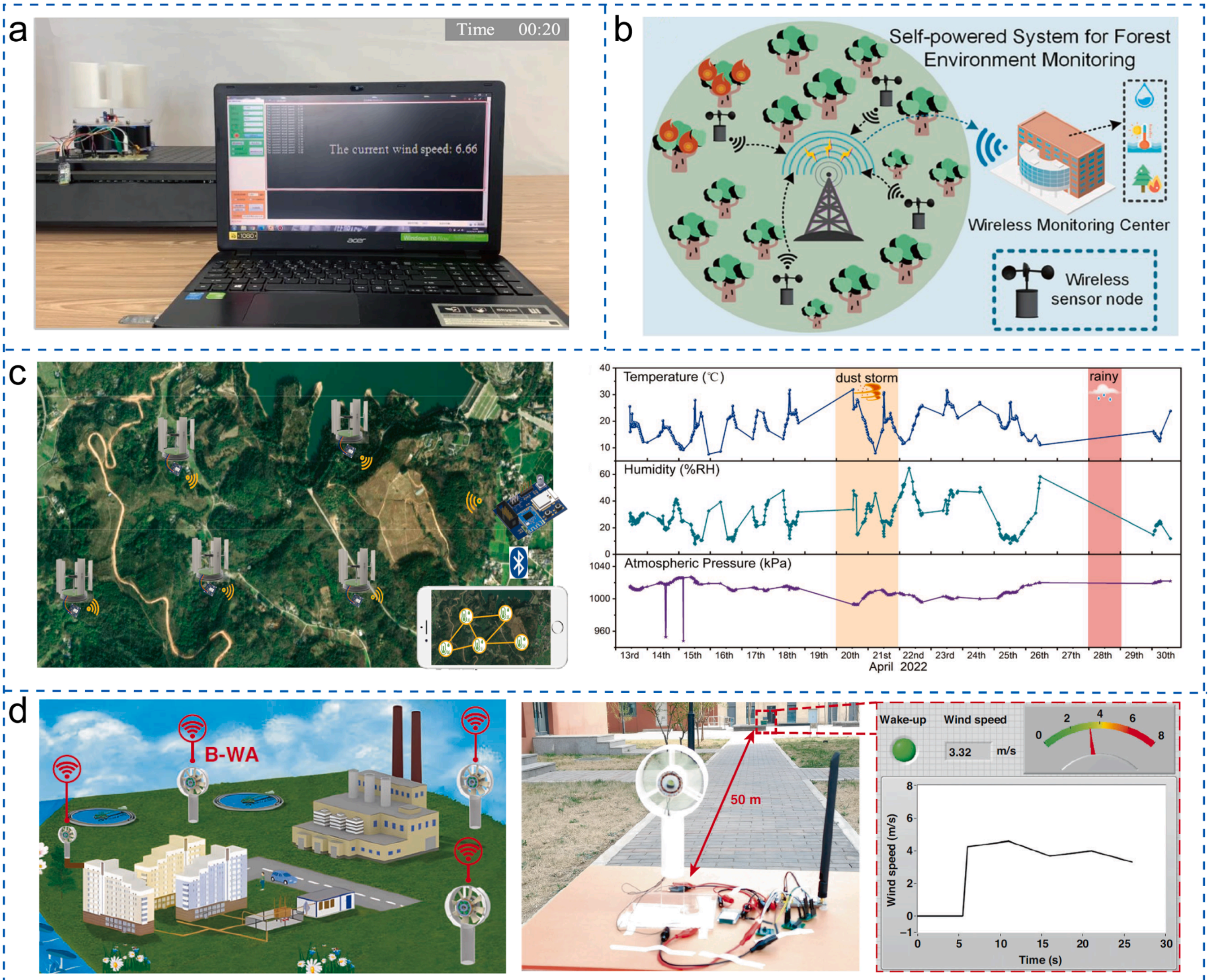

Fig. 13. IoT application of wind-TENG in wireless environmental monitoring area. (a) Demonstration of self-powered wind speed measurement and wireless transmission based on Bluetooth [102]. (b) Illustration of self-powered wireless sensor nodes based on the hybrid wind nanogenerator realizing a self-powered forest environment monitoring microsystem [105]. (c) Distributed wireless temperature, humidity, and atmospheric pressure monitoring nodes with a communication length of 2.1 km driven by wind-TENG [21]. (d) Application prospects of the TENG-based anemometer in intelligent environmental monitoring and a photograph of the TENG-based anemometer in an outdoor environment [60].
Reproduced with permission.

wireless technology. To accelerate energy harvesting, a hybrid Wind-TENG-EMG system was employed. By integrating a humidity and temperature sensor, the system is capable of forest fire monitoring. After 13 s, a 1000 μF capacitor can be charged to 3.4 V, which can power the wireless node to work automatically. The switch will turn off automatically when the capacitor voltage falls below 2 V, restarting the charging process. Moreover, the TENG-powered system can operate continuously at a wind speed of 8–9 m/s.

However, Bluetooth and Zigbee have communication distance limitations of approximately 100 m, often reduced to around 50 m in practical use. To overcome this, researchers have pursued longer transmission distances with limited energy. Liu et al. [21] developed a self-powered distributed environment monitoring node based on Sub-1G (433 MHz) wireless frequency, capable of sensing temperature, humidity, and atmospheric pressure (Fig. 13c). Nine sensing nodes are distributed around the receiver, with distances ranging from 100 m to 2.1 kilometers. With a low start-up wind speed, the sensing nodes successfully provided continuous monitoring for over half a month, capturing variations in temperature, dust storms, and rainfall during the spring season. Fu et al. [60] also designed a similar Sub-1G frequency-based wind speed detection system (Fig. 13d), with operational power ranging from 30 nW (static power) to 121 mW (data transmission moment). With a start-up wind speed of 2 m/s, the system achieved 50-meter data transmission under natural conditions.

Up to now, wind-TENGs are capable of charging millifarad capacitors to 3.3 V or 5 V in several minutes, enabling wireless environmental monitoring over distances of several kilometers[106,107]. A more ambitious application is wireless GPS monitoring [35], which holds potential for remote and untraversed area monitoring, such as mountain fire monitoring [108], ocean monitoring, and human location.

6. Summary and discussion

In this review, the recent progress of TENGs in wind energy harvesting has been comprehensively summarized, from its basic theory to practical applications. From the perspective of wind-TENGs' practicability, natural wind distribution and annual wind speed statistics are investigated firstly. The output characteristics and four working modes of TENGs in wind energy harvesting are also analyzed in detail. Additionally, the recent progress of wind-TENGs in terms of structural design and start-up wind speed are summarized. Furthermore, the integration of power management circuits and wind-TENGs for optimizing energy collection efficiency is discussed. Finally, three major application fields based on wind-TENGs are presented, including agriculture, transportation, and environmental monitoring.

The use of power management circuits and automatic switches has proven effective in enabling self-powered systems. Although significant progress has been made in the technological applications of the wind-TENG, several challenges and issues remain that need to be addressed for the future development of this research field.

For device design, the challenges for practicability include: (1) Durability and longevity. On the one hand, the high voltage probably makes the materials carbonized causing a short lifetime. On the other hand, the harsh outdoor environments (e.g. dusty, hurricane) and the frictional resistance will cause heavy material wear. Further work is anticipated to develop more robust triboelectric materials and structure designs that can withstand continuous operation over several years. (2) Optimized design for low wind conditions. Various efforts, such as flexible slim film usage and tiny contact structure design, have been made to reduce wind resistance but with inferior output performance. Further, other methods, such as polarization as well as surface modification, can improve this problem with better output performance, but the performance can not be maintained for a long time. Developed structural designs with stable high-output performance and low start-up wind speed are anticipated to address this dilemma.

For power management circuits, the challenges might be: (1) Universal power management circuit. The unique output characteristics of every single TENG require customized power management circuit designs, which causes many repetitive works. Since the wind-TENG output is within a predictable range, a universal power management circuit is anticipated to be developed to enhance practicability. (2) Energy storage loss. Leakage current exists anytime in all the circuit components causing an energy storage loss. Since the wind energy input is intermittent, the system becomes non-functional when the energy loss is higher than the energy input. Current studies seldom mention this real-world problem but it is a non-negligible issue for practical application. Choosing the components with lower current leakage and high sub-threshold swing is an effective approach for now, and further energy leakage prevention strategies should be explored to improve the performance of the power management circuit.

For applications, the challenges might be: (1) Intelligent energy allocation. As an energy harvester, to date, one wind-TENG can power around 4000 series LEDs directly, and it is also able to power sensors and devices with microwatt or milliwatt consumption such as bulbs, air pressure sensors, temperature sensors, PH sensors, calculators, hygrothemometers, etc. by saving the energy into a capacitor. Even the applications of wireless communication (Bluetooth, Zigbee, Sub-1G, GPS, etc.) have high energy consumption, the wind-TENG can power them up intermittently by saving the energy into the capacitor for a longer time. However, such loads can not be powered all the time. In this case, it is crucial to construct an intelligent energy allocation strategy, for example smart load match [104], for achieving an unintermittent working system. (2) More sensing scenarios. As for the wind-TENG-based sensors, wind-speed sensors are the most commonly employed. That is because the TENG outputs a signal with unstable amplitude but stable phases. The phase is directly correlated with the rotational speed/contact frequency corresponding to the wind speed. Given the current limitations in wind-TENG-based sensing design, more sensing scenarios could be explored such as rotation displacement and rotation circles by expanding the wind-TENG design.

Additionally, for better practical wind-TENG development, some other challenges need to be addressed: (1) Scaling up for industrial applications. While TENGs excel in small-scale, low-power applications, scaling them up to harvest wind energy on a larger, industrial scale remains a challenge. Innovations in material science, device architecture, and energy management are necessary for wind-TENGs to achieve higher power densities. (2) Cost-effectiveness and commercial viability. Although TENGs can be manufactured using low-cost materials, their cost-effectiveness at scale requires further evaluation. Commercial viability will depend on reducing production costs, improving efficiency, and making TENG systems economically competitive with other renewable energy technologies, such as photovoltaic cells and traditional wind turbines. (3) Environmental and aesthetic impact. For large-scale deployment in urban or natural environments, minimizing the environmental and aesthetic impact of wind-TENGs is also important. Designing unobtrusive, visually appealing devices that can be integrated seamlessly into buildings, streets, or ecosystems will be important for public acceptance and widespread adoption. (4) Combination with artificial intelligence (AI) technology, biotechnology [109], and other cutting-edge technologies. Since AI will become the most important technology shortly, it is critical to make a good combination between AI and TENG to promote the development of both. For example, TENG can be used to construct a low-power AI system, and AI technology can also be used to analyze the self-powered sensing data intelligently [110]. (5) Theoretical breakthrough. We believe the mechanism needs further exploration to improve energy conversion efficiency. The high charge density generation with less frictional force needs to be studied, which can improve the ability of micro-energy harvesting and the lifetime of the TENG device. On the other hand, how to extract more energy from the TENG lessening the impact of high inherent impedance needs a theoretical breakthrough.

In summary, TENG as a promising wind energy harvesting technology plays a critical role in the future's energy supplement due to its abundance, ubiquitous, and renewable. However, its erratic and intermittent characteristics simultaneously limit its utility. For further practical applications, more efforts need to be made in device design (including structure design, materials optimization, etc.), circuit design, and energy allocation. Moreover, based on TENG technology, combining various energy sources such as solar and ocean energy together might be a potential approach in the near future.

CRediT authorship contribution statement

Wang Zhong Lin: Supervision, Methodology, Conceptualization. **Ji Minglan:** Writing – review & editing, Resources, Investigation. **Kang Jiahao:** Writing – review & editing, Visualization, Supervision, Project administration, Funding acquisition, Formal analysis. **Luo Jianjun:** Writing – review & editing, Resources, Investigation. **Liu Di:** Writing – original draft, Visualization, Methodology, Investigation, Funding acquisition, Formal analysis, Data curation. **Chen Muqi:** Writing – review & editing, Resources, Investigation. **Huang Lijun:** Writing – review & editing, Resources, Investigation.

Declaration of Competing Interest

The authors declare that they have no known competing financial interests or personal relationships that could have appeared to influence the work reported in this paper.

Acknowledgement

This research was supported by National Key R&D Program of China (No. 2023YFB3211200) and the China Postdoctoral Science Foundation (No. 2023M740050).

Data availability

No data was used for the research described in the article.

References

[1] X. Cao, Y. Xiong, J. Sun, X. Xie, Q. Sun, Z.L. Wang, Multidiscipline applications of triboelectric nanogenerators for the intelligent era of internet of things, Nanomicro Lett. 15 (2022) 14, https://doi.org/10.1007/s40820-022-00981-8.

[2] B. Shi, Q. Wang, H. Su, J. Li, B. Xie, P. Wang, J. Qiu, C. Wu, Y. Zhang, X. Zhou, T. W. Kim, Progress in recent research on the design and use of triboelectric nanogenerators for harvesting wind energy, Nano Energy 116 (2023) 108789, https://doi.org/10.1016/j.nanoen.2023.108789.

[3] D. Wöhrle, D. Meissner, Organic solar cells, Adv. Mater. 3 (2004) 129–138, https://doi.org/10.1002/adma.19910030303.

[4] A. Haroun, M. Tarek, M. Mosleh, F. Ismail, Recent progress on triboelectric nanogenerators for vibration energy harvesting and vibration sensing, Nanomaterials 12 (17) (2022), https://doi.org/10.3390/nano12172960.

[5] J. Luo, Z. Wang, L. Xu, A.C. Wang, K. Han, T. Jiang, Q. Lai, Y. Bai, W. Tang, F. R. Fan, Z.L. Wang, Flexible and durable wood-based triboelectric nanogenerators for self-powered sensing in athletic big data analytics, Nat. Commun. 10 (2019) 5147, https://doi.org/10.1038/s41467-019-13166-6.

[6] Y. Yang, B. Chen, Z.L. Wang, Scavenging wind energy by triboelectric nanogenerators, Adv. Energy Mater. 8 (2018) 1702649, https://doi.org/10.1002/aenm.201702649.

[7] K. Turoń, Hydrogen-powered vehicles in urban transport systems-current state and development, Trans. Res. Procedia 45 (2020) 835, https://doi.org/10.1016/j.trpro.2020.02.086.

[8] P. McKendry, Energy production from biomass, Bioresour. Technol. 83 (2002) 37, https://doi.org/10.1016/S0960-8524(01)00118-3.

[9] M. Leijon, O. Danielsson, M. Eriksson, K. Thorburn, H. Bernhoff, J. Isberg, J. Sundberg, I. Ivanova, E. Sjöstedt, O. Ågren, K.E. Karlsson, A. Wolfbrandt, An electrical approach to wave energy conversion, Renew. Energy 31 (2006) 1309–1319, https://doi.org/10.1016/j.renene.2005.07.009.

[10] M. Ali, S.A. Khan, Shamsuddin, A. Ali, S. Ali, R. ul Hassan, D.H. Cho, D. Byun, Low profile wind savonius turbine triboelectric nanogenerator for powering small electronics, Sens. Actuators A Phys. 363 (2023) 114535, https://doi.org/10.1016/j.sna.2023.114535.

[11] C. Zhang, W. Tang, C. Han, F. Fan, Z.L. Wang, Theoretical comparison, equivalent transformation, and conjunction operations of electromagnetic induction generator and triboelectric nanogenerator for harvesting mechanical energy, Adv. Mater. 26 (2014) 3580–3591, https://doi.org/10.1002/adma.201400207.

[12] F.R. Fan, Z.Q. Tian, Z. Lin Wang, Flexible triboelectric generator, Nano Energy 1 (2012) 328–334, https://doi.org/10.1016/j.nanoen.2012.01.004.

[13] Z.L. Wang, On Maxwell's displacement current for energy and sensors: the origin of nanogenerators, Mater. Today 20 (2017) 74–82, https://doi.org/10.1016/j.mattod.2016.12.001.

[14] J. Zhao, G. Zhen, G. Liu, T. Bu, W. Liu, X. Fu, P. Zhang, C. Zhang, Z.L. Wang, Remarkable merits of triboelectric nanogenerator than electromagnetic generator for harvesting small-amplitude mechanical energy, Nano Energy 61 (2019) 111–118, https://doi.org/10.1016/j.nanoen.2019.04.047.

[15] L. Zu, D. Liu, J. Shao, Y. Liu, S. Shu, C. Li, X. Shi, B. Chen, Z.L. Wang, A self-powered early warning glove with integrated elastic-arched triboelectric nanogenerator and flexible printed circuit for real-time safety protection, Adv. Mater. Technol. 7 (2021) 2100787, https://doi.org/10.1002/admt.202100787.

[16] Y. Zi, H. Guo, Z. Wen, M.-H. Yeh, C. Hu, Z.L. Wang, Harvesting low-frequency (< 5 Hz) irregular mechanical energy: a possible killer application of triboelectric nanogenerator, ACS Nano 10 (2016) 4797–4805, https://doi.org/10.1021/acsnano.6b01569.

[17] Y. Yang, G. Zhu, H. Zhang, J. Chen, X. Zhong, Z. Lin, Y. Su, P. Bai, X. Wen, Z. L. Wang, Triboelectric nanogenerator for harvesting wind energy and as self-powered wind vector sensor system, ACS Nano 7 (2013) 9461, https://doi.org/10.1021/nn4043157.

[18] Y.C. Lai, Y.C. Hsiao, H.M. Wu, Z.L. Wang, Waterproof fabric-based multifunctional triboelectric nanogenerator for universally harvesting energy from raindrops, wind, and human motions and as self-powered sensors, Adv. Sci. 6 (2019) 1801883, https://doi.org/10.1002/advs.201801883.

[19] B. Zhang, C. Zhang, O. Yang, W. Yuan, Y. Liu, L. He, Y. Hu, Z. Zhao, L. Zhou, J. Wang, Z.L. Wang, Self-powered seawater electrolysis based on a triboelectric nanogenerator for hydrogen production, ACS Nano 16 (2022) 15286–15296, https://doi.org/10.1021/acsnano.2c06701.

[20] P. Chen, J. An, R. Cheng, S. Shu, A. Berbille, T. Jiang, Z.L. Wang, Rationally segmented triboelectric nanogenerator with a constant direct-current output and low crest factor, Energy Environ. Sci. 14 (2021) 4523–4532, https://doi.org/10.1039/D1EE01382C.

[21] D. Liu, C. Li, P. Chen, X. Zhao, W. Tang, Z.L. Wang, Sustainable long-term and wide-area environment monitoring network based on distributed self-powered wireless sensing nodes, Adv. Energy Mater. 13 (2022) 2202691, https://doi.org/10.1002/aenm.202202691.

[22] K. Han, J. Luo, Y. Feng, Q. Lai, Y. Bai, W. Tang, Z.L. Wang, Wind-driven radial-engine-shaped triboelectric nanogenerators for self-powered absorption and degradation of nox, ACS Nano 14 (2020) 2751–2759, https://doi.org/10.1021/acsnano.9b08496.

[23] Y. Xie, S. Wang, L. Lin, Q. Jing, Z. Lin, S. Niu, Z. Wu, Z.L. Wang, Rotary triboelectric nanogenerator based on a hybridized mechanism for harvesting wind energy, ACS Nano 7 (2013) 71192012, https://doi.org/10.1021/nn402477h.

[24] Z.L. Wang, Self-powered nanosensors and nanosystems, Adv. Mater. 24 (2012) 280–285, https://doi.org/10.1002/adma.201102958.

[25] X. Cao, H. Zhou, Y. Zhou, Y. Hu, Y. Wang, Z.L. Wang, Q. Sun, High performance rotary-structured triboelectric-electromagnetic hybrid nanogenerator for ocean wind energy harvesting, Adv. Mater. Technol. 8 (2023) 2300327, https://doi.org/10.1002/admt.202300327.

[26] Y. Fang, T. Tang, Y. Li, C. Hou, F. Wen, Z. Yang, T. Chen, L. Sun, H. Liu, C. Lee, A high-performance triboelectric-electromagnetic hybrid wind energy harvester based on rotational tapered rollers aiming at outdoor IoT applications, iScience 24 (2021) 102300, https://doi.org/10.1016/j.isci.2021.102300.

[27] A. Ghaffarinejad, J.Y. Hasani, R. Hinchet, Y. Lu, H. Zhang, A. Karami, D. Galayko, S.W. Kim, P. Basset, A conditioning circuit with exponential enhancement of output energy for triboelectric nanogenerator, Nano Energy 51 (2018) 173–184, https://doi.org/10.1016/j.nanoen.2018.06.034.

[28] W. Harmon, D. Bamgboje, H. Guo, T. Hu, Z.L. Wang, Self-driven power management system for triboelectric nanogenerators, Nano Energy 71 (2020) 104642, https://doi.org/10.1016/j.nanoen.2020.104642.

[29] J. Bae, J. Lee, S. Kim, J. Ha, B. Lee, Y. Park, C. Choong, J. Kim, Z.L. Wang, H. Kim, J. Park, U. Chung, Flutter-driven triboelectrification for harvesting wind energy, Nat. Commun. 5 (2014) 4929–4937, https://doi.org/10.1038/ncomms5929.

[30] Q. Li, W. Liu, H. Yang, W. He, L. Long, M. Wu, X. Zhang, Y. Xi, C. Hu, Z.L. Wang, Ultra-stability high-voltage triboelectric nanogenerator designed by ternary dielectric triboelectrification with partial soft-contact and non-contact mode, Nano Energy 90 (2021) 106585, https://doi.org/10.1016/j.nanoen.2021.106585.

[31] H. Wang, L. Xu, Y. Bai, Z.L. Wang, Pumping up the charge density of a triboelectric nanogenerator by charge-shuttling, Nat. Commun. 11 (2020) 4203, https://doi.org/10.1038/s41467-020-17891-1.

[32] J. Wang, W. Ding, L. Pan, C. Wu, H. Yu, L. Yang, R. Liao, Z.L. Wang, Self-powered wind sensor system for detecting wind speed and direction based on a triboelectric nanogenerator, ACS Nano 12 (2018) 3954–3963, https://doi.org/10.1021/acsnano.8b01532.

[33] Y. Wang, T. Chen, S. Sun, X. Liu, Z. Hu, Z. Lian, L. Liu, Q. Shi, H. Wang, J. Mi, T. Zhou, C. Lee, M. Xu, A humidity resistant and high performance triboelectric nanogenerator enabled by vortex-induced vibration for scavenging wind energy, Nano Res. 15 (2021) 3246–3253, https://doi.org/10.1007/s12274-021-3968-9.

[34] W. Yan, Y. Liu, P. Chen, L.N.Y. Cao, J. An, T. Jiang, W. Tang, B. Chen, Z.L. Wang, Flexible film-discharge-switch assisted universal power management system for the four operation modes of triboelectric nanogenerators, Adv. Energy Mater. 12 (2022) 2103677, https://doi.org/10.1002/aenm.202103677.

[35] Y. Zhang, X. Gao, Y. Zhang, J. Gui, C. Sun, H. Zheng, S. Guo, High-efficiency self-charging power systems based on performance-enhanced hybrid nanogenerators and asymmetric supercapacitors for outdoor search and rescue, Nano Energy 92 (2022) 106788, https://doi.org/10.1016/j.nanoen.2021.106788.

[36] J. Luo, W. Gao, Z.L. Wang, The triboelectric nanogenerator as an innovative technology toward intelligent sports, Adv. Mater. 33 (2021) 2004178, https://doi.org/10.1002/adma.202004178.

[37] J. Luo, Z.L. Wang, Recent progress of triboelectric nanogenerators: from fundamental theory to practical applications, EcoMat 2 (2020) e12059, https://doi.org/10.1002/eom2.12059.

[38] S. Niu, Z.L. Wang, Theoretical systems of triboelectric nanogenerators, Nano Energy 14 (2015) 161–192, https://doi.org/10.1016/j.nanoen.2014.11.034.

[39] J. Shao, M. Willatzen, T. Jiang, W. Tang, X. Chen, J. Wang, Z.L. Wang, Quantifying the power output and structural figure-of-merits of triboelectric nanogenerators in a charging system starting from the Maxwell's displacement current, Nano Energy 59 (2019) 380–389, https://doi.org/10.1016/j.nanoen.2019.02.051.

[40] S. Niu, S. Wang, L. Lin, Y. Liu, Y.S. Zhou, Y. Hu, Z.L. Wang, Theoretical study of contact-mode triboelectric nanogenerators as an effective power source, Energy Environ. Sci. 6 (2013) 3576–3583, https://doi.org/10.1039/C3EE42571A.

[41] J. Li, J. Chen, H. Guo, Triboelectric nanogenerators for harvesting wind energy: recent advances and future perspectives, Energies 14 (2021) 6949, https://doi.org/10.3390/en14216949.

[42] M. Willatzen, Z. Lin Wang, Theory of contact electrification: optical transitions in two-level systems, Nano Energy 52 (2018) 517–523, https://doi.org/10.1016/j.nanoen.2018.08.015.

[43] S. Wang, X. Mu, X. Wang, A.Y. Gu, Z.L. Wang, Y. Yang, Elasto-aerodynamics-driven triboelectric nanogenerator for scavenging air-flow energy, ACS Nano 9 (2015) 9554–9563, https://doi.org/10.1021/acsnano.5b04396.

[44] M.A.M. Hasan, W. Zhu, C.R. Bowen, Z.L. Wang, Y. Yang, Triboelectric nanogenerators for wind energy harvesting, Nat. Rev. Electr. Eng. 1 (2024) 453–465, https://doi.org/10.1038/s44287-024-00061-6.

[45] C.L. Archer, M.Z. Jacobson, Evaluation of global wind power, J. Geophys. Res. Atmos. 110 (2005), https://doi.org/10.1029/2004JD005462.

[46] H.J. Ko, D.S. Kwon, K. Bae, J. Kim, Self-suspended shell-based triboelectric nanogenerator for omnidirectional wind-energy harvesting, Nano Energy 96 (2022) 107062, https://doi.org/10.1016/j.nanoen.2022.107062.

[47] L. Zhang, B. Meng, Y. Tian, X. Meng, X. Lin, Y. He, C. Xing, H. Dai, L. Wang, Vortex-induced vibration triboelectric nanogenerator for low speed wind energy harvesting, Nano Energy 95 (2022) 107029, https://doi.org/10.1016/j.nanoen.2022.107029.

[48] Y. Tian, X. Meng, X. Lin, L. Zhang, C. Xing, H. Dai, L. Wang, Z. Peng, B. Meng, A dual auxiliary beam galloping triboelectric nanogenerator for low speed wind energy harvesting, Appl. Phys. Lett. 121 (2022) 093902, https://doi.org/10.1063/5.0107120.

[49] Z. Ren, Z. Wang, Z. Liu, L. Wang, H. Guo, L. Li, S. Li, X. Chen, W. Tang, Z.L. Wang, Energy harvesting from breeze wind (0.7–6 m s^{-1}) using ultra-stretchable

triboelectric nanogenerator, Adv. Energy Mater. 10 (2020) 2001770, https://doi.org/10.1002/aenm.202001770.
[50] S. Cho, D. Lee, S. Jang, S. Cho, J. Shim, Y. Jang, Z.H. Lin, K. Choi, D. Choi, Physical intelligence-based working mode adaptable triboelectric nanogenerator for effective wind energy harvesting in broad range, Nano Energy 113 (2023) 108608, https://doi.org/10.1016/j.nanoen.2023.108608.
[51] Z. Lin, B. Zhang, H. Guo, Z. Wu, H. Zou, J. Yang, Z.L. Wang, Super-robust and frequency-multiplied triboelectric nanogenerator for efficient harvesting water and wind energy, Nano Energy 64 (2019) 103908, https://doi.org/10.1016/j.nanoen.2019.103908.
[52] Z. Zhao, X. Pu, C. Du, L. Li, C. Jiang, W. Hu, Z.L. Wang, Freestanding flag-type triboelectric nanogenerator for harvesting high-altitude wind energy from arbitrary directions, ACS Nano 10 (2016) 1780–1787, https://doi.org/10.1021/acsnano.5b07157.
[53] O. Gulahmadov, M.B. Muradov, J. Kim, The wind-driven Scotch yoke-based triboelectric nanogenerator system for energy harvesting, Int. J. Energy Res. 46 (2022) 10989–10997, https://doi.org/10.1002/er.7900.
[54] X. Fu, S. Xu, Y. Gao, X. Zhang, G. Liu, H. Zhou, Y. Lv, C. Zhang, Z.L. Wang, Breeze-wind-energy-powered autonomous wireless anemometer based on rolling contact-electrification, ACS Energy Lett. 6 (2021) 2343–2350, https://doi.org/10.1021/acsenergylett.1c00704.
[55] X. Fu, Y. Qin, Z. Zhang, G. Liu, J. Cao, B. Fan, Z. Wang, Z. Wang, C. Zhang, Ultra-robust and high-performance rotational triboelectric nanogenerator by bearing charge pumping, Energy Environ. Mater. 7 (2023) e12566, https://doi.org/10.1002/eem2.12566.
[56] S. Yong, J. Wang, L. Yang, H. Wang, H. Luo, R. Liao, Z.L. Wang, Auto-switching self-powered system for efficient broad-band wind energy harvesting based on dual-rotation shaft triboelectric nanogenerator, Adv. Energy Mater. 11 (2021) 2101194, https://doi.org/10.1002/aenm.202101194.
[57] H. Li, J. Wen, Z. Ou, E. Su, F. Xing, Y. Yang, Y. Sun, Z.L. Wang, B. Chen, Leaf-like tengs for harvesting gentle wind energy at an air velocity as low as 0.2 m s^{-1}, Adv. Funct. Mater. 33 (2023) 2212207, https://doi.org/10.1002/adfm.202212207.
[58] S. Yuan, Q. Zeng, D. Tan, Y. Luo, X. Zhang, H. Guo, X. Wang, Z.L. Wang, Scavenging breeze wind energy (1–8.1 m s^{-1}) by minimalist triboelectric nanogenerator based on the wake galloping phenomenon, Nano Energy 100 (2022) 107465, https://doi.org/10.1016/j.nanoen.2022.107465.
[59] L. Zhang, B. Meng, Y. Xia, Z. Deng, H. Dai, P. Hagedorn, Z. Peng, L. Wang, Galloping triboelectric nanogenerator for energy harvesting under low wind speed, Nano Energy 70 (2020) 104477, https://doi.org/10.1016/j.nanoen.2020.104477.
[60] X. Fu, Z. Jiang, J. Cao, Z. Dong, G. Liu, M. Zhu, C. Zhang, A near-zero quiescent power breeze wake-up anemometer based on a rolling-bearing triboelectric nanogenerator, Microsyst. Nanoeng. 10 (2024) 51, https://doi.org/10.1038/s41378-024-00676-7.
[61] J. Han, Y. Feng, P. Chen, X. Liang, H. Pang, T. Jiang, Z.L. Wang, Wind-driven soft-contact rotary triboelectric nanogenerator based on rabbit fur with high performance and durability for smart farming, Adv. Funct. Mater. 32 (2021) 2108580, https://doi.org/10.1002/adfm.202108580.
[62] M. Olsen, R. Zhang, J. Örtegren, H. Andersson, Y. Yang, H. Olin, Frequency and voltage response of a wind-driven fluttering triboelectric nanogenerator, Sci. Rep. 9 (2019) 5543, https://doi.org/10.1038/s41598-019-42128-7.
[63] J.H. Son, D. Heo, D. Goh, M. Lee, J. Chung, S. Choi, S. Lee, Wind-driven bidirectional fluttering triboelectric nanogenerator via dual flagpole and slot structure design, Adv. Mater. Technol. 8 (2023) 2200453, https://doi.org/10.1002/admt.202200453.
[64] X. Li, Y. Cao, X. Yu, Y. Xu, Y. Yang, S. Liu, T. Cheng, Z.L. Wang, Breeze-driven triboelectric nanogenerator for wind energy harvesting and application in smart agriculture, Appl. Energy 306 (2022) 117977, https://doi.org/10.1016/j.apenergy.2021.117977.
[65] H. Lin, M. He, Q. Jing, W. Yang, S. Wang, Y. Liu, Y. Zhang, J. Li, N. Li, Y. Ma, L. Wang, Y. Xie, Angle-shaped triboelectric nanogenerator for harvesting environmental wind energy, Nano Energy 56 (2019) 269–276, https://doi.org/10.1016/j.nanoen.2018.11.037.
[66] K. Zhao, J. Meng, M. Zhong, S. Li, Y. Niu, H. Liu, B.N. Gu, M.J. Liu, D. Zhang, L. Kong, Y.L. Chueh, Design of a self-powered system by wind-driven triboelectric nanogenerator based on 0.94(Bi0.5Na0.5)TiO3-0.06Ba(Zr0.25Ti0.75)O3/polyvinylidene fluoride (bnt-bzt/pvdf) composites, Small 18 (2022) 2202792, https://doi.org/10.1002/smll.202202792.
[67] J.S. Lee, H. Yong, Y.I. Choi, J. Ryu, S. Lee, Stackable disk-shaped triboelectric nanogenerator to generate energy from omnidirectional wind, Int. J. Precis. Eng. Manuf.-Green Technol. 9 (2021) 557–565, https://doi.org/10.1007/s40684-021-00340-9.
[68] Q. Mu, W. He, C. Shan, S. Fu, S. Du, J. Wang, Z. Wang, K. Li, C. Hu, Achieving high-efficiency wind energy harvesting triboelectric nanogenerator by coupling soft contact, charge space accumulation, and charge dissipation design, Adv. Funct. Mater. 34 (2023) 2309421, https://doi.org/10.1002/adfm.202309421.
[69] K. Zhao, W. Sun, X. Zhang, J. Meng, M. Zhong, L. Qiang, M.J. Liu, B.N. Gu, C. C. Chung, M. Liu, F. Yu, Y.L. Chueh, High-performance and long-cycle life of triboelectric nanogenerator using PVC/MoS2 composite membranes for wind energy scavenging application, Nano Energy 91 (2022) 106649, https://doi.org/10.1016/j.nanoen.2021.106649.
[70] Q. Han, Z. Ding, W. Sun, X. Xu, F. Chu, Hybrid triboelectric-electromagnetic generator for self-powered wind speed and direction detection, Sustain. Energy Technol. 39 (2020) 100717, https://doi.org/10.1016/j.seta.2020.100717.
[71] M.T. Rahman, M. Salauddin, J.Y. Park, A natural wind-driven 3d-printed miniaturized and fully enclosed hybrid nanogenerator using flexible blade structure for subway tunnel applications, in: Proceedings of the 20th Int. Solid-State Sen. Actuators Microsyst. Conf., 2019, 1443. ⟨https://ieeexplore.ieee.org/document/8808321⟩.
[72] M.T. Rahman, S.M.S. Rana, P. Maharjan, M. Salauddin, T. Bhatta, H. Cho, C. Park, J.Y. Park, Ultra-robust and broadband rotary hybridized nanogenerator for self-sustained smart-farming applications, Nano Energy 85 (2021) 105974, https://doi.org/10.1016/j.nanoen.2021.105974.
[73] Y. Luo, P. Chen, L.N.Y. Cao, Z. Xu, Y. Wu, G. He, T. Jiang, Z.L. Wang, Durability improvement of breeze-driven triboelectric-electromagnetic hybrid nanogenerator by a travel-controlled approach, Adv. Funct. Mater. 32 (2022) 2207510, https://doi.org/10.1002/adfm.202205710.
[74] S. Yong, H. Wang, Z. Lin, X. Li, B. Zhu, L. Yang, W. Ding, R. Liao, J. Wang, Z. L. Wang, Environmental self-adaptive wind energy harvesting technology for self-powered system by triboelectric-electromagnetic hybridized nanogenerator with dual-channel power management topology, Adv. Energy Mater. 12 (2022) 2202468, https://doi.org/10.1002/aenm.202202469.
[75] C. Ye, K. Dong, J. An, J. Yi, X. Peng, C. Ning, Z.L. Wang, A triboelectric–electromagnetic hybrid nanogenerator with broadband working range for wind energy harvesting and a self-powered wind speed sensor, Acs Energy Lett. 6 (2021) 1143–1152, https://doi.org/10.1021/acsenergylett.1c00244.
[76] X. Fan, J. He, J. Mu, J. Qian, N. Zhang, C. Yang, X. Hou, W. Geng, X. Wang, X. Chou, Triboelectric-electromagnetic hybrid nanogenerator driven by wind for self-powered wireless transmission in Internet of Things and self-powered wind speed sensor, Nano Energy 68 (2020) 104319, https://doi.org/10.1016/j.nanoen.2019.104319.
[77] X. Cheng, W. Tang, Y. Song, H. Chen, H. Zhang, Z.L. Wang, Power management and effective energy storage of pulsed output from triboelectric nanogenerator, Nano Energy 61 (2019) 517–532, https://doi.org/10.1016/j.nanoen.2019.04.096.
[78] X. Liang, T. Jiang, Y. Feng, P. Lu, J. An, Z.L. Wang, Triboelectric nanogenerator network integrated with charge excitation circuit for effective water wave energy harvesting, Adv. Energy Mater. 10 (2020) 2002123, https://doi.org/10.1002/aenm.202002123.
[79] L. Xu, T.Z. Bu, X.D. Yang, C. Zhang, Z.L. Wang, Ultrahigh charge density realized by charge pumping at ambient conditions for triboelectric nanogenerators, Nano Energy 49 (2018) 625–633, https://doi.org/10.1016/j.nanoen.2018.05.011.
[80] W. Liu, Z. Wang, G. Wang, G. Liu, J. Chen, X. Pu, Y. Xi, X. Wang, H. Guo, C. Hu, Z. L. Wang, Integrated charge excitation triboelectric nanogenerator, Nat. Commun. 10 (2019) 1426, https://doi.org/10.1038/s41467-019-09464-8.
[81] S.H. Chung, J. h Son, K. Cha, M. Choi, H. Jung, M.K. Kim, J. Hong, S. Lee, Boosting power output of fluttering triboelectric nanogenerator based on charge excitation through multi-utilization of wind, Nano Energy 111 (2023) 108389, https://doi.org/10.1016/j.nanoen.2023.108389.
[82] S. Farhangi, U. Kirchenberger, D. Schroeder, Energy based closed form solution of ZCS multiresonant series parallel converters, IEEE Trans. Power Electron. 11 (1996) 285–291. ⟨https://ieeexplore.ieee.org/document/486177⟩.
[83] M.M. McQuage, V.P. McDowell, F.E. Peterkin, J.A. Pasour, High power density capacitor charging power supply development for repetitive pulsed power, in: Proceedings of the 27th Int. Power Modulator Conf., 2006, 368. ⟨https://ieeexplore.ieee.org/document/4216213⟩.
[84] X. Xia, X. Zhang, Y. Yu, H. Li, B. Zhang, M. He, Y. Wang, X. Lu, T. Cheng, An energy-coupled triboelectric nanogenerator based on charge pump for wind and water environments, Energy Convers. Manag. 312 (2024) 118569, https://doi.org/10.1016/j.enconman.2024.118569.
[85] H. Qin, G. Gu, W. Shang, H. Luo, W. Zhang, P. Cui, B. Zhang, J. Guo, G. Cheng, Z. Du, A universal and passive power management circuit with high efficiency for pulsed triboelectric nanogenerator, Nano Energy 68 (2020) 104372, https://doi.org/10.1016/j.nanoen.2019.104372.
[86] Z. Zhang, G. Gu, W. Zhang, Z. Du, G. Cheng, Triboelectric nanogenerator with enhanced charge density and limited open-circuit voltage for efficient power management and industrial environmental monitoring, Nano Energy 131 (2024) 110308, https://doi.org/10.1016/j.nanoen.2024.110308.
[87] F. Xi, Y. Pang, W. Li, T. Jiang, L. Zhang, T. Guo, G. Liu, C. Zhang, Z.L. Wang, Universal power management strategy for triboelectric nanogenerator, Nano Energy 37 (2017) 168–176, https://doi.org/10.1016/j.nanoen.2017.05.027.
[88] X. Cheng, L. Miao, Y. Song, Z. Su, H. Chen, X. Chen, J. Zhang, H. Zhang, High efficiency power management and charge boosting strategy for a triboelectric nanogenerator, Nano Energy 38 (2017) 438–446, https://doi.org/10.1016/j.nanoen.2017.05.063.
[89] S. Niu, X. Wang, F. Yi, Y.S. Zhou, Z.L. Wang, A universal self-charging system driven by random biomechanical energy for sustainable operation of mobile electronics, Nat. Commun. 6 (2015) 8975, https://doi.org/10.1038/ncomms9975.
[90] W. Wang, Y. Shang, K. Han, X. Shi, T. Jiang, W. Mai, J. Luo, Z.L. Wang, Self-powered agricultural product preservation and wireless monitoring based on dual-functional triboelectric nanogenerator, ACS Appl. Mater. Interfaces 16 (2024) 20642–20651, https://doi.org/10.1021/acsami.4c02869.
[91] Z. Wang, Q. Tang, C. Shan, Y. Du, W. He, S. Fu, G. Li, A. Liu, W. Liu, C. Hu, Giant performance improvement of triboelectric nanogenerator systems achieved by matched inductor design, Energy Environ. Sci. 14 (2021) 6627–6637, https://doi.org/10.1039/D1EE02852A.

[92] Y. Zhou, P. Lu, X. Zhou, J. Bai, S. An, S. Liu, X. Pu, Triboelectric wind sensors: fundamentals, progress, and perspectives, Nano Energy 131 (2024) 110209, https://doi.org/10.1016/j.nanoen.2024.110209.
[93] X. Li, J. Luo, K. Han, X. Shi, Z. Ren, Y. Xi, Y. Ying, J. Ping, Z.L. Wang, Stimulation of ambient energy generated electric field on crop plant growth, Nat. Food 3 (2022) 133–142, https://doi.org/10.1038/s43016-021-00449-9.
[94] K. Han, J. Luo, J. Chen, B. Chen, L. Xu, Y. Feng, W. Tang, Z.L. Wang, Self-powered ammonia synthesis under ambient conditions via N2 discharge driven by Tesla turbine triboelectric nanogenerators, Microsyst. Nanoeng. 7 (2021) 7, https://doi.org/10.1038/s41378-020-00235-w.
[95] S. Wang, Y. Liu, K. Zhang, S. Gao, Self-powered electrocatalytic nitrate to ammonia driven by lightweight triboelectric nanogenerators for wind energy harvesting, Nano Energy 112 (2023) 108434, https://doi.org/10.1016/j.nanoen.2023.108434.
[96] J. Luo, K. Han, X. Wu, H. Cai, T. Jiang, H. Zhou, Z.L. Wang, Self-powered mobile sterilization and infection control system, Nano Energy 88 (2021) 106313, https://doi.org/10.1016/j.nanoen.2021.106313.
[97] S. Jeon, S. Kim, S. Park, M. Seol, D. Kim, Y. Chang, Y. Choi, Self-powered electro-coagulation system driven by a wind energy harvesting triboelectric nanogenerator for decentralized water treatment, Nano Energy 28 (2016) 288–295, https://doi.org/10.1016/j.nanoen.2016.08.051.
[98] J. Jiang, Y. Zhang, Q. Shen, Q. Zhu, X. Ge, Y. Liu, Z. Wen, X. Sun, A self-powered hydrogen leakage sensor based on impedance adjustable windmill-like triboelectric nanogenerator, Nano Energy 89 (2021) 106453, https://doi.org/10.1016/j.nanoen.2021.106453.
[99] E. Su, H. Li, J. Zhang, Z. Xu, B. Chen, L.N.Y. Cao, Z.L. Wang, Rationally designed anti-glare panel arrays as highway wind energy harvester, Adv. Funct. Mater. 33 (2023) 2214934, https://doi.org/10.1002/adfm.202214934.
[100] C. Zhang, Y. Liu, B. Zhang, O. Yang, W. Yuan, L. He, X. Wei, J. Wang, Z.L. Wang, Harvesting wind energy by a triboelectric nanogenerator for an intelligent high-speed train system, ACS Energy Lett. 6 (2021) 1490–1499, https://doi.org/10.1021/acsenergylett.1c00368.
[101] T. Du, F. Dong, M. Zhu, Z. Xi, F. Li, Y. Zou, P. Sun, M. Xu, Self-powered and robust marine exhaust gas flow sensor based on bearing type triboelectric nanogenerator, J. Mar. Sci. Eng. 10 (2022) 1416, https://doi.org/10.3390/jmse10101416.
[102] H. Zou, L. Zhao, Q. Wang, Q. Gao, G. Yan, K. Wei, W. Zhang, A self-regulation strategy for triboelectric nanogenerator and self-powered wind-speed sensor, Nano Energy 95 (2022) 106990, https://doi.org/10.1016/j.nanoen.2022.106990.
[103] D. Liu, B. Chen, J. An, C. Li, G. Liu, J. Shao, W. Tang, C. Zhang, Z.L. Wang, A self-regulation strategy for triboelectric nanogenerator and self-powered wind-speed sensor, Nano Energy 73 (2020) 104819, https://doi.org/10.1016/j.nanoen.2022.106990.
[104] K. Sou, Z. Lin, Y. Jin, S. Ping, W. Ding, J. Wang, A hybrid wind and raindrop energy harvesting operating on Savonius turbine, Nano Energy 127 (2024) 109746, https://doi.org/10.1016/j.nanoen.2024.109746.
[105] B. Li, Y. Qiu, P. Huang, W. Tang, X. Zhang, Self-powered forest ambient monitoring microsystem based on wind energy hybrid nanogenerators, Sci. China Technol. Sci. 65 (2022) 2348–2360, https://doi.org/10.1007/s11431-022-2167-2.
[106] L. Xu, L. Xu, J. Luo, Y. Yan, B.E. Jia, X. Yang, Y. Gao, Z.L. Wang, Hybrid all-in-one power source based on high-performance spherical triboelectric nanogenerators for harvesting environmental energy, Adv. Energy Mater. 10 (2020) 2001669, https://doi.org/10.1002/aenm.202001669.
[107] H. Zhang, J. Wang, Y. Xie, G. Yao, Z. Yan, L. Huang, S. Chen, T. Pan, L. Wang, Y. Su, W. Yang, Y. Lin, Self-powered, wireless, remote meteorologic monitoring based on triboelectric nanogenerator operated by scavenging wind energy, ACS Appl. Mater. Interfaces 8 (2016) 32649–32654, https://doi.org/10.1021/acsami.6b12798.
[108] Y. Cao, E. Su, Y. Sun, Z.L. Wang, L. Cao, A Rolling-Bead Triboelectric Nanogenerator for Harvesting Omnidirectional Wind-Induced Energy toward Shelter Forests Monitoring, Small 20 (2024) 2307119, https://doi.org/10.1002/smll.202307119.
[109] X. Zhou, G. Li, D. Wu, H. Liang, W. Zhang, L. Zeng, Q. Zhu, P. Lai, Z. Wen, C. Yang, Y. Pan, Recent advances of cellular stimulation with triboelectric nanogenerators, Exploration 3 (2023) 20220090, https://doi.org/10.1002/EXP.20220090.
[110] J. Hu, C. Fan, M. Tang, H. Chen, H. Pan, Z. Zhang, N. Yang, Artificial intelligence enabled self-powered sensing and wind energy harvesting system for bridges monitoring, Nano Energy 132 (2024) 110349, https://doi.org/10.1016/j.nanoen.2024.110349.